

CHAPTER 1

INTRODUCTION

1.1 Introduction

Topical delivery system has been introduced to prevent or treat a wide variety of diseases, especially diseases related to skin. It is also widely used to deliver cosmeceutical active ingredients into skin in order to maintain, improve and nourish the physical outlook of human being. Topical products are mostly intended for the localized effects at the site of their application by virtue of drug penetration into the underlying layers of skin or mucous membranes (Mehta, 2000). Drugs and active ingredients could be delivered through a variety of topical formulations including creams, lotions, ointments, gels, solutions, suspensions, pastes, sprays and transdermal patches.

There are number of advantages for drug administration via topical route as compared with other administrations. One of the main reasons is to avoid the first pass metabolism and gastrointestinal disturbances (Gaur *et al.*, 2013). For example, metformin, the first-line oral anti-diabetic drug, has been reported for causing abdominal discomfort, nausea and diarrhoea during the treatment (Nyenwe *et al.*, 2011). Therefore, topical or transdermal delivery of metformin is one of the possible administration route that could minimize its side effect.

Although oral administration is generally the simplest, most convenient and economical route, it is nevertheless problematic because of the unpredictable nature of gastrointestinal drug absorption (Raffa, 2010). Some drugs have low oral bioavailability as they do not practically well absorb by gastrointestinal mucosa. Alteration of any physiological environment, for example, as a result of change in diet, lifestyle, age or health status, also affect drug absorption and bioavailability (Raffa, 2010). The presence of nutrients and foodstuffs in the gastrointestinal tract can affect the absorption of a drug by binding to it or by altering the physiologic environment such as pH of the stomach and intestines. For example, the penicillin V and tetracycline administered orally with food will not be well absorbed (Finkel *et al.*, 1981) due to the interactions

between food components and drugs, thus hinder the antimicrobial efficacy of those agents (Watson, 1986).

The intravenous administration delivers the drug directly into the bloodstream and gives the fastest effect to the patient. However, this type of administration is inconvenient for the patient and practitioner. In the case of diabetic patient for instance, daily injection of insulin will cause painful suffering. This will definitely reduce the patient compliances especially to the younger patients. At this junction, topical delivery offers ease of application and minimizes the risk of infection via intravenous administration (Kwatra *et al.*, 2012; Moody, 2010). An alternative to intravenous administration, diabetes patient could avoid daily injection by applying anti-diabetic transdermal patch which improved the patient compliances and reduced the painfulness and risk of infection (Paudel *et al.*, 2010).

Topical delivery could be another alternative route for those drugs that may cause adverse effect at high dosage. Topical application allows the drugs to be delivered in a controlled release rate through the skin as compared to direct injection of the drugs into the systemic circulation. The controlled release property of topical delivery could minimize the adverse effect of certain drugs.

Topical application of medicines has obvious advantages in the management of localized disease. Topical corticosteroids for example can be applied topically at desired site and work effectively in managing dermatitis (Maia *et al.*, 2000). Anesthetic drugs such as lidocaine and benzocaine will give a local analgesic effect when directly applied on ulcers or inflammation site (Sobanko *et al.*, 2012).

However, there are imminent challenges for certain drugs or active compounds to be topically applied through skin. This is because of the barrier property of skin limited the absorption of a wide range of substances. Therefore, the understanding of the skin structure and its function is especially important.

1.2 The Structure and Function of Skin

Skin is the largest organ of the human body with an average surface area of 1.7 m² and contributes around 10% of the body weight (Edwards & Marks, 1995; Williams, 2003). This outermost surface of human body is preventing the ingress of harmful chemicals and microorganisms whilst regulating heat and water loss from body (Brisson, 1974). It is also functions as sense organ via various receptors for temperature, pain and touch. In addition, it acts as a physical barrier to the environment and providing protection against mechanical insults (Wiechers, 1989).

Skin comprises three main distinct layers (Figure 1.1), namely epidermis, dermis and hypodermis (from outermost to innermost layer) (Lai-Cheong & McGrath, 2013). Epidermis is the outermost multiply layered membrane without blood vessels. The thickness of epidermis varies from 0.06 mm on the eyelids to around 0.8 mm on the soles of the feet and palms of the hand (Arda *et al.*, 2014). Epidermis contains four separate layers (Figure 1.1), from the outside to inside, are the stratum corneum, stratum granulosum, stratum spinosum and the stratum basale (Geerligs, 2010). These four histologically distinct layers are formed by the differing stages of the keratinocyte maturation (Williams, 2003).

The uppermost layer of epidermis, stratum corneum is the final product of keratinocyte maturation and made up of the layers of hexagonal-shaped, non-viable cornified cells which known as corneocytes (Bensouilah & Buck, 2006). In stratum corneum, corneocytes are surrounded by a cell envelope composed of cross-linked proteins and embedded in lipid lamellar regions, which are oriented parallel to the corneocytes surface, thereby providing the epidermis with a water impermeable barrier (Brisson, 1974; Krutmann & Humbert, 2011; Williams, 2003). Generally, the stratum corneum comprises 15 to 20 cell layers with an average thickness around 15 µm (Brisson, 1974). The stratum corneum layer plays an essential role in maintaining and

structuring the lipid barrier which affords protection against external insults and water loss through the skin (Zaidi & Lanigan, 2010). The unique resulting structure of stratum corneum has a key role provides the physical barrier for topical and transdermal delivery of a wide range of substances.

The stratum granulosum consists of 1 to 5 layers of flattened polygonal granulated cells which undergo final cell differentiation, synthesizes the keratin and starts to flatten (Arda *et al.*, 2014; Williams, 2003). At this stage of differentiation, the degradation of the viable cell components such as the nuclei and organelles is apparent and the cytoplasm of the flattened cells becomes increasingly filled with keratohyalin masses and filaments (Geerligs, 2010).

Stratum spinosum is the thicker cell membrane that consists of 2 to 6 rows of keratinocytes which change the morphology from columnar to polygonal cells (Williams, 2003). It is formed when the keratinocytes reproduced and matured.

Stratum basale is the basal layer of epidermis which lies adjacent to the dermis and mainly comprised of keratinocytes. The presence of melanocytes which synthesise the pigment melanin from tyrosine (Kanitakis, 2002) gives the colour of skin and provides protection against ultraviolet (UV) radiation (Lai-Cheong & McGrath, 2013) at this layer.

Dermis is the major component of skin which composed of a dense network of elastic tissue and collagen fibres (Lai-Cheong & McGrath, 2013). This elastic network is providing support and flexibility of human skin (Wilkes *et al.*, 1973). The thickness of dermis is ranging from 1 mm to 4 mm (Smoller & Hiatt, 2009). Blood vessels, nerves, lymph vessels and skin appendages such as sweat glands, sebaceous glands and hairs are located in the dermis (Figure 1.1). The extensive vasculature supplies blood flow to dermis for regulation of body temperature, delivers nutrients and oxygen to tissue and also removing the toxins and waste products.

The innermost layer, hypodermis also called subcutaneous fat layer which is mainly composed of adipose tissue that spreads all over the body with the exception of the eyelids (Barry, 1983). This sheet of fat layer lies between the overlying dermis and the underlying body constituents. The thickness of the hypodermis varies with the age, gender, nutritional status and physical conditions of the individual. This fatty layer of skin principally serves to insulate the body and acts as mechanical cushion against the physical shock. It is also a site that provides a readily available supply of high energy molecules for human body.

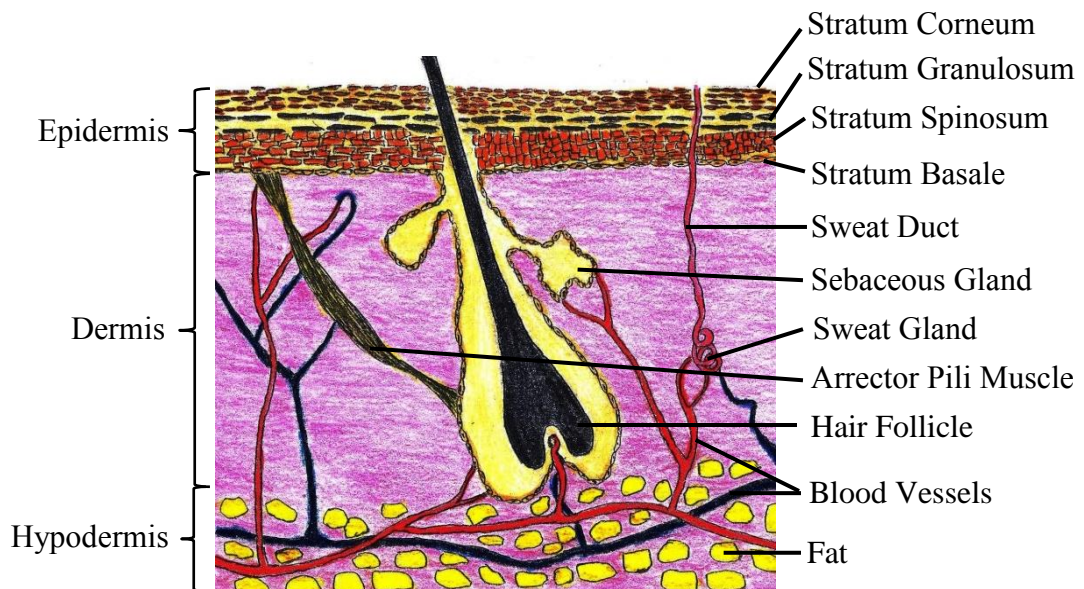


Figure 1.1: Illustration of cross-section through human skin adapted from reference (Williams, 2003).

1.3 Lipid Nanoparticles

Lipid nanoparticles are nano-sized colloidal particles that composed by lipid and stabilized by surfactants (Pardeike *et al.*, 2009). They are derived from o/w emulsions by replacing the liquid oil with solid lipid (Jenning *et al.*, 2000). Since the starting materials are lipids in solid form, lipid nanoparticles present as rigid particles and being solid at both room temperature and body temperature.

Lipid particles have been used in pharmaceutical application for long time and the first fat emulsion namely *Intralipid* was developed by Wretling *et al.* and used for parenteral nutrition (Vinnars & Hammarqvist, 2004). This early innovation had opened a new chapter in the development especially delivery of lipophilic drugs. Some products based on this system like *Etomidate*, *Diazumuls* and *Lipofundin* MCT/LCT had successfully been marketed (Davis *et al.*, 1987; Graham *et al.*, 1977; Müller & Heinemann, 1994). In the early of nineties, the submicron size of lipid particles were reported by Speiser *et al.* as “Lipid nanopellets” (Speiser, 1990). This study has opened up new ideas in which emphasizing the nanotechnology in preparation of lipid particles. Later, Müller and his co-workers successfully prepared the lipid nanoparticles by using the high pressure homogenization technique (Müller *et al.*, 1995) and then patented this invention in 1991 (Lucks & Müller, 1991). Gasco and his co-workers also developed and filed another patent describing the preparation of SLN via microemulsion technique (Gasco, 1993).

1.3.1 Solid Lipid Nanoparticles

Solid lipid nanoparticles (SLN) have initially been studied by Müller *et al.* as an alternative carrier system to emulsion, liposomes, polymeric nanoparticles (Pardeike *et al.*, 2009). Unlike emulsion, the SLNs were produced by replacing the liquid oil of the emulsion with single or mixture of solid lipids. Therefore, SLN are mostly solid particles with a mean particle size between 40 nm to 1000 nm (Lucks & Müller, 1991). In the early stage of SLN research, it was initially focused on pharmaceutical applications such as oral and parenteral administration (Wissing *et al.*, 2004), and later the interest of SLN research gradually shifted to the topical and transdermal applications (Guimarães & Rê 2011).

SLNs are beneficial in many aspects such as able to minimize the usage of organic solvents, possess negligible toxicity, ease of encapsulation for the lipophilic substances, provide protection for incorporated actives and able to increase bioavailability of lipophilic compounds (Das *et al.*, 2012; Müller *et al.*, 1995). Moreover, the solid matrix nature of SLN has the property of sustained release of drugs or active ingredients (Mühlen *et al.*, 1998). SLNs are also possible to penetrate through skin by manifesting its particle size (Priano *et al.*, 2007).

Although this type of carrier has demonstrated several advantages as excipient, it does have some limitations especially of low encapsulation capacity and possible expulsion of drug from the matrix during storage. Normally, the preparation of lipid nanoparticles involved rapid recrystallization process. The lipid nanoparticles produced generally considered less ordered crystal structured (Souto *et al.*, 2006), therefore mostly are not stable and tend to transform into more ordered crystal during storage (Awad *et al.*, 2009). This rearrangement of the crystal structure could reduce the

accommodation spaces in the particles that led to the drug or active ingredient exclusion (Jenning & Gohla, 2001).

1.3.2 Nanostructured Lipid Carriers

Due to some limitations of SLN, development of new generation of lipid nanoparticles has led into what so called nanostructured lipid carriers (NLC) (Das *et al.*, 2012) which as a result of certain amount of liquid lipid or oil were mixed with solid lipid in order to improve the encapsulation efficiency and reduce drug expulsion (Jenning *et al.*, 2000). The mixing of liquid oil with solid lipid could lead to a massive crystal lattice disturbance and therefore creates enough space to accommodate drug molecules, thereby improves the encapsulation efficiency of active compounds (Souto *et al.*, 2004; Jennings & Gohla, 2001).

1.4 Preparation of Lipid Nanoparticles

Many different techniques for the preparation of lipid nanoparticles (SLN and NLC) have been reported in the literatures (Mehnert & Mäder, 2012). Among these techniques, the high pressure homogenization, microemulsion technique and melt-emulsification combine ultrasonication method were the popular approaches that used in preparation of lipid nanoparticles (Anton *et al.*, 2008; Pardeike *et al.*, 2009). Basically all the SLN and NLC preparation methods involved two step processes, *i.e.* the formation of o/w lipid nanoemulsion and subsequently recrystallization to obtain the nanoparticles.

1.4.1 High Pressure Homogenization

High pressure homogenization technique has extensively been investigated for the preparation of SLN and NLC. Lipid nanoparticles can be prepared by either the hot or cold high pressure homogenization technique. In the hot homogenization method, molten solid lipid for SLN or mix of solid and liquid lipids for NLC with the active ingredients was dispersed in a pre-heated surfactant solution. This mixture was emulsified by high speed stirring and then passed through a high pressure homogenizer adjusted to the same temperature. The obtained lipid nanoemulsions were left to cool down in room temperature.

In cold homogenization method, the molten lipid with active ingredients was cooled down to room temperature. After solidification, the lipid was ground to obtain lipid granules and then dispersed in a cold surfactant solution. This mixture was passed through the high pressure homogenizer at room temperature to yield nano-sized lipid particles.

High pressure homogenization technique avoids the use of toxic organic solvents and less quantities of water content. Moreover, high pressure homogenization is widely used in the production of emulsion for parenteral nutrition in the pharmaceutical industry. Therefore, this technique is possible to produce SLN and NLC in industry scale. However, this technique has high possibility to degrade the chemically labile actives due to the critical preparation condition (high temperature and pressure).

1.4.2 Microemulsion Technique

Microemulsion can be defined as isotropic and thermodynamically stable o/w or w/o dispersion stabilized by emulsifier(s) (Mozafari, 2006). Gasco and his co-workers have developed the preparation of SLN through microemulsion technique (Gasco, 1993) by mixing a molten lipid with surfactant, co-surfactant generally medium chain alcohols such as butanol and water. This hot microemulsion is then dispersed in large amount of cold water with stirring. The cooling process leads to rapid recrystallization of the microemulsion, thus forming the lipid nanoparticles.

Although this preparation method do not require high mechanical energy used in the formation of nanoparticles, however it is not very practical because the use of medium chain alcohol may cause toxicity and irritation (Tenjarla, 1999). In addition, the total lipid content in lipid nanoparticles was considerably low due to large amount of water used in the cooling process (Mehnert & Mäder, 2012).

1.4.3 Melt-Emulsification Combined with Ultrasonication Method

In the melt-emulsification combined with ultrasonication method for the preparation of lipid nanoparticles was initially developed by Domb *et al.* (Domb & Maniar, 1991). This preparation starts with the dispersion of drug in the molten lipid and subsequently mixed with the pre-heated surfactant solution. This mixture was homogenized with high speed homogenizer to form emulsion and further sonicated with ultrasonicator to form nanoemulsion. Subsequently, the prepared nanoemulsion was dispersed in cold water for recrystallization of the lipid nanoparticles.

Homogenizer and ultrasonicator are mostly readily accessible equipments, thus makes this preparation method becomes one of the popular approach in SLN and NLC researches. In general, this method presents a good potential for lipid nanoparticle preparation because the formulation parameters are directly controllable. Hence, melt-emulsification combined with ultrasonication method was used in this study to prepare the lipid nanoparticles in this study.

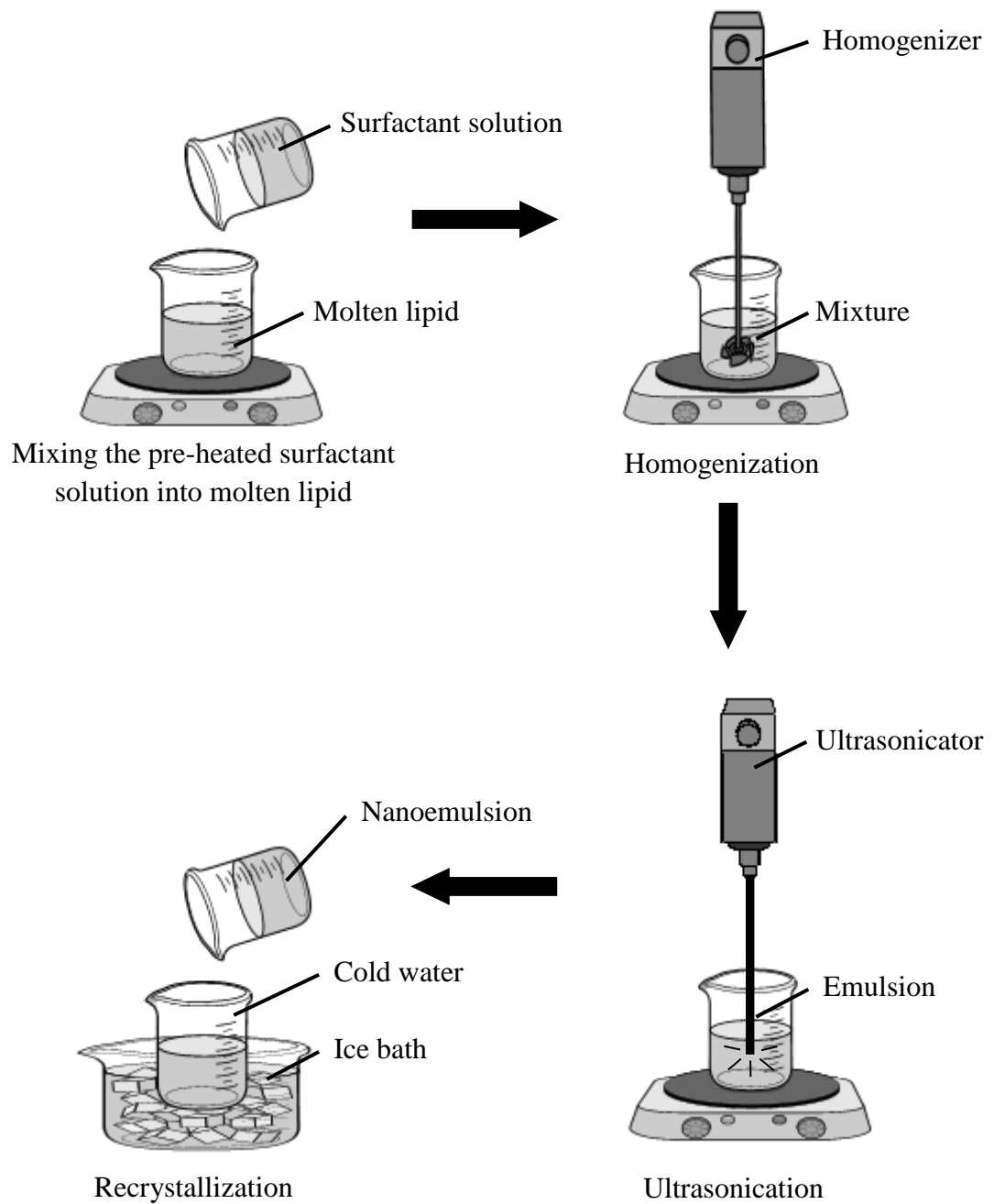


Figure 1.2: Schematic diagram of melt-emulsification combine with ultrasonication method for preparation of lipid nanoparticles.

1.5 Materials Used in Formulation of Lipid Nanoparticles

SLN and NLC can be prepared from different types of starting material such as triglycerides, phospholipids and waxes (Han *et al.*, 2008; Jennings *et al.*, 2000; Kheradmandnia *et al.*, 2010; Tsai *et al.*, 2012). Among them, fatty acid is one of the most cost effective raw materials and therefore has widely been used in order to reduce the production cost. Hence, fatty acids were used as raw materials in the preparation of lipid nanoparticles in order to develop cost effective carrier system. In this present work, a series of stearic acid lipid nanoparticles incorporated with different ratio of oleic acid were prepared and named stearic-oleic acid nanoparticles (SONs).

1.5.1 Fatty Acids

Fatty acids are the main components in the preparation of SONs. They are a class of monocarboxylic acid with a hydrocarbon chain, which is either saturated or unsaturated or branched. In this work, fatty acids with single hydrocarbon chain were chosen in the preparation of lipid nanoparticles. Generally, fatty acids have the hydrocarbon chain with even number of carbon atoms in natural sources. Fatty acids present in the form of ester in triglycerides, phospholipids and glycolipids. They are the important energy source for our body. Fatty acids are metabolized in our body to obtain a large amount of adenosine-5'-triphosphate (ATP) to supply energy for our daily activities (Mangold, 1995).

The chemical and physical properties of fatty acids are varying with their occurrences. Saturated fatty acids exist as powder or solid form in room temperature whereas unsaturated fatty acids appear in liquid form even both fatty acid molecules having same number of carbon atoms. Unsaturated fatty acids with one or more double bonds in their hydrocarbon chains and can occur in *cis* or *trans* configuration. The

natural unsaturated fatty acids obtained in plants have double bond with *cis* configuration whereas the synthetic fatty acids generally occur in *trans* configuration.

Fatty acids can be categorized into several groups based on their fatty acid chain length (Mangold, 1995):

- Short-chain fatty acids are fatty acids with hydrocarbon chain of fewer than six carbons;
- Medium-chain fatty acids are fatty acids with aliphatic tails of 6 to 12 carbons;
- Long-chain fatty acids are fatty acids with hydrocarbon chain of more than 12 carbons.

Essential fatty acids are fatty acids required in human body but cannot be generated by ourselves (Simopoulos, 1991). Therefore, essential fatty acids have to be consumed from food. The important sources to obtain essential fatty acids are from plant oils and fish oils. Examples of essential fatty acids are linoleic acid, linolenic acid, arachidonic acid and others.

Stearic acid and oleic acid were used to produce SONs in this work because they are non-toxic, biocompatible with our body, cost effective and easily obtain from plants especially palm oil. This also would be an additional value for oil palm products.

Stearic acid (Figure 1.3) is the saturated carboxylic acid with a hydrocarbon chain consists of 18 carbon atoms and has the IUPAC name called octadecanoic acid. Its name comes from the Greek word “*st áur*”, meaning tallow and was first described by Chevreul *et al.* in 1823 (Leray, 2012). Its empirical formula is $C_{18}H_{36}O_2$ with molar mass of $284.48 \text{ g mol}^{-1}$. It appears as shiny white flakes or powder and very slightly soluble in water. Its melting point is at $69\text{-}70 \text{ }^\circ\text{C}$ and boiling point at $383 \text{ }^\circ\text{C}$.

Stearic acid occurs as glycerol ester in animal and vegetable fats where it is one of the most abundant long chain saturated fatty acid that found in nature. It is the major composition of cocoa butter (33.2%) and beef tallow (18.9%) also can be obtained from palm oil (4.4%) and palm kernel oil (2.8%) in Malaysia (Denke, 1994). Stearic acid is widely used as ingredient in making candles, soaps, plastics, lubricant, cosmetics and pharmaceutical products.

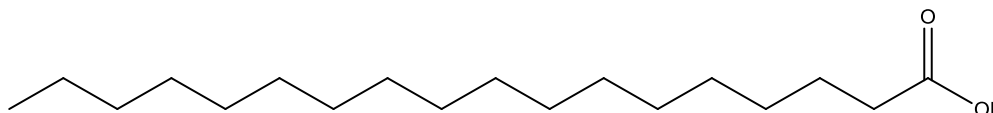


Figure 1.3: Molecular structure of stearic acid (octadecanoic acid).

Oleic acid (Figure 1.4) is the monounsaturated fatty acid consists of a single hydrocarbon chain with 18 carbon atoms and one *cis* double bond that located between 9th and 10th carbon atom. Its molecular formula is $C_{18}H_{34}O_2$ with molar mass of $282.42 \text{ g mol}^{-1}$. It was also discovered by Chevreul *et al.* in his pioneering studies on pork fat in 1823 (Stillwell, 2013). Oleic acid presents as colourless oil at room temperature and insoluble in water. The melting point of pure oleic acid is at $4 \text{ }^\circ\text{C}$ and boiling point at $286 \text{ }^\circ\text{C}$.

Oleic acid is abundantly found in the form of glycerol ester in vegetable oils and also can exist in the form of ethyl ester in animals and man (Leray, 2012). The sources of oleic acid for human consumption are olive oil (about 60-70%), nut oils, canola oil, sesame oil, cocoa butter, lard, palm oil and soybean oil (Leray, 2012).

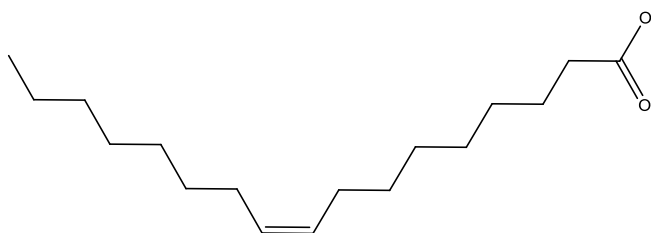


Figure 1.4: Molecular structure of oleic acid (*cis*-9-octadecenoic acid).

1.5.2 Surfactants

Surface active agents or surfactants are one of the important components in preparation of SONs because they functioned as emulsifier in the emulsification process and stabilizer for nanoparticles. Surfactants are amphiphilic molecules that consist of non-polar hydrophobic portion, usually a straight or branched hydrocarbon chain containing 8 to 18 carbon atoms with or without C=C double bonds, which is attached to a polar or ionic functional group (hydrophilic). The polar or ionic head group interacts strongly with water molecules, whereas the non-polar hydrocarbon chain interacts strongly with organic molecules. Due to this amphiphilic characteristic, surfactant has the ability to adsorb at the interface when present at low concentration altering the interfacial energies of interfaces (boundary between any immiscible phases). The general illustration of surfactants is shown in Figure 1.5.

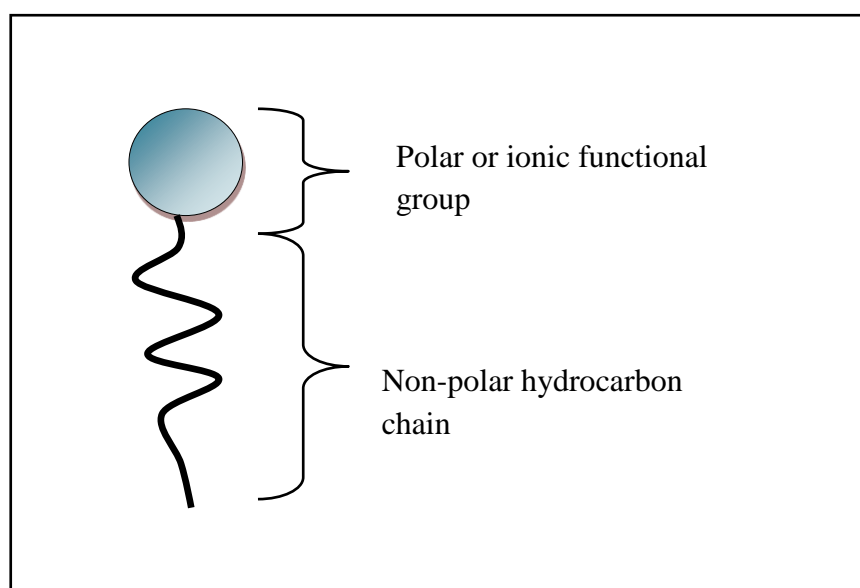


Figure 1.5: Schematic diagram of a surface active agent.

Surfactants can be classified based on their nature of polar head group namely categorised as anionic, cationic, amphoteric and non-ionic (Tadros, 2006). Anionic surfactants are the surfactants with the anionic functional group attached with non-polar

hydrocarbon chain. They are the most widely used surfactants in laundry industry due to their low production cost and practically compatible in every type of detergents.

The most common cationic surfactants are quaternary ammonium compounds with alkyl group such as cetyl trimethylammonium bromide (Table 1.1). They were widely used in hair conditioner, softener, antistatic agents and bactericides due to their positive charges on the polar head group able to adsorb at negatively charged surface.

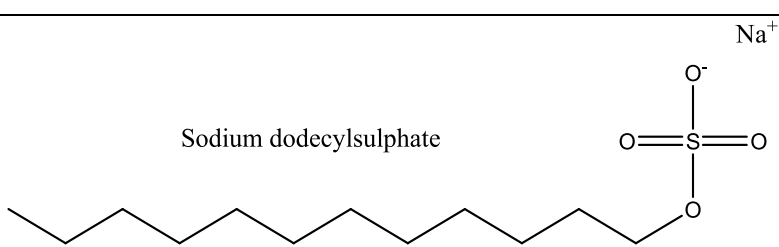
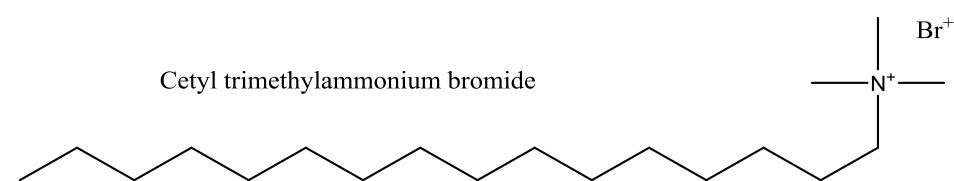
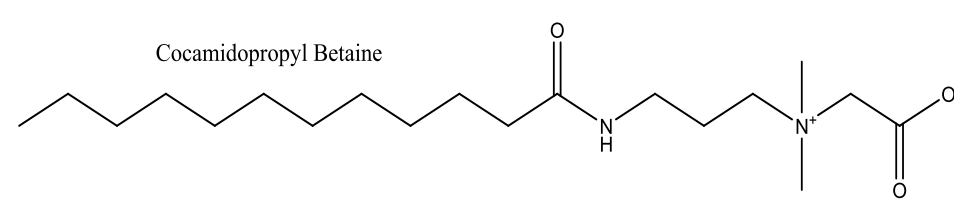
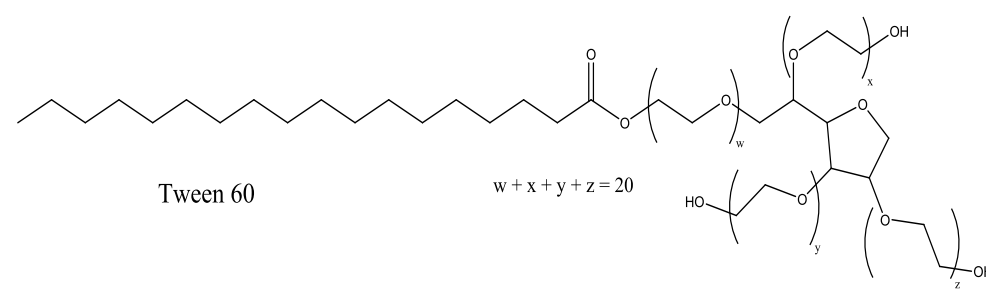
Amphoteric or zwitterionic surfactants are surfactants containing both cationic and anionic functional groups. N-alkyl betaines (Table 1.1) are the common example of this class of surfactants. They have isoelectric property where the molecules become positive charge in low pH, whereas they behave like anionic surfactants in alkaline solution. They were frequently used in personal care products because of low eye irritation.

Non-ionic surfactants are also widely used in food, cosmetic and pharmaceutical industries because of its low toxicity, less irritation to eye and mild to skin. They can be distinguished to several classes: sorbitan ester ethoxylates, alcohol ethoxylates, monoalkylamide ethoxylates, glycol esters, glucosides, sucrose esters, polymeric surfactants and others (Tadros, 2006).

The non-ionic surfactants that used in preparation of SONs were ethoxylated fatty acid esters of sorbitan (Tweens). Tweens type surfactants were commonly used in cosmetic and pharmaceutical industries, sometime even in food industry. Tweens are ethoxylated derivative of fatty acid ester of sorbitan (Span). The hydroxyl moieties on sorbitan esters could react with ethylene oxide to produce Tweens. Generally, they have a bulky polar head group which contained twenty units of ethylene oxides. The polyethylene moieties of Tweens change the lipophilic property of sorbitan esters to hydrophilic and increased the number of HLB of Tweens. In addition, the polyethylene

moieties of Tweens make them appear as viscous liquid at room temperature. The bulky polar head group of Tweens has relatively high steric effect to stabilize the emulsion droplets. Tween type surfactants can further react with fatty acid to form polyethylene sorbitan di- or tri-esters, but sorbitan tri-esters are more common to be used in food, cosmetic and pharmaceutical industries (Tadros, 2006). Molecular structure of Tween 60 is shown in Table 1.1.

Table 1.1: Examples of different types of surfactants that commonly used in cosmetic and pharmaceutical industries.

Surfactant Type	Example
Anionic	<p>Sodium dodecylsulphate</p> 
Cationic	<p>Cetyl trimethylammonium bromide</p> 
Zwitterionic	<p>Cocamidopropyl Betaine</p> 
Nonionic	<p>Tween 60</p> <p>$w + x + y + z = 20$</p> 

1.6 Lipid Nanoparticles as Advanced Topical Delivery System

Topical application has widely been used as delivery system for cosmetic and pharmaceutical application. However, the conventional topical formulation (*e.g.* emulsion) normally associated with low uptake due to the barrier function of the stratum corneum and potential absorption to the systemic circulation (Benson, 2000; Jayaraman *et al.*, 1996; Jennings *et al.*, 2000) that make it a complex system. Therefore, lipid nanoparticles were introduced as advanced topical delivery systems in order to minimise these problems (Pardeike *et al.*, 2009). Lipid nanoparticles have extensively been investigated as delivery system especially for cosmetic and pharmaceutical applications. A wide range of substances has been incorporated into lipid nanoparticles for topical formulation. Example of these active ingredients and drugs are summarised in Table 1.2.

Table 1.2: Examples of active ingredients and drugs incorporated into lipid nanoparticles for topical application.

Incorporated Active Ingredients and Drugs	Application	Reference
Ascorbyl palmitate	Antioxidant	Üner <i>et al.</i> , 2005
Benzocaine	Anaesthetic agent	Puglia <i>et al.</i> , 2011
Butylmethoxydibenzoyl methane	UV filter	Scalia <i>et al.</i> , 2011
Clotrimazole	Antifungal agent	Souto <i>et al.</i> , 2004
Coenzyme Q10	Antioxidant	Teeranachaideekul <i>et al.</i> , 2007
Glucocorticoids	Dermatitis	Maia <i>et al.</i> , 2000
Ketoconazole	Antifungal agent	Ramasamy <i>et al.</i> , 2012
Lidocaine	Anaesthetic agent	Pathak & Nagarsenker, 2009
Retinoic Acid	Acne treatment	Castro <i>et al.</i> , 2007

Lipid nanoparticles have been used for dermal application due to many advantages features of these carrier systems over conventional formulation such as it occurs as rigid particles at both room temperature and body temperature, enhances percutaneous absorption and prolongs release of its payload. As discussed at Section 1.2, stratum corneum is the physical barrier of skin that limits the percutaneous absorption of active substances into the skin. Lipid nanoparticles have been developed as one of the approaches to improve skin penetration of active ingredients. Pardeike *et al.* reported that the coenzyme Q10 loaded in NLC has higher skin penetration as compared to liquid paraffin and emulsion (Pardeike & Müller, 2007). Moreover, Schwarz *et al.* in their work proved that smaller particles improved the skin penetration by manifesting the particle size of coenzyme Q10 loaded NLC to ultra-small size (<100 nm) (Schwarz *et al.*, 2013). However, the penetration of active ingredients through skin was also affected by the composition of lipid nanoparticles (Schlupp *et al.*, 2011).

Numerous studies have shown that lipid nanoparticles have the ability for prolong release of its payloads (Hu *et al.*, 2005; Puglia *et al.*, 2011; Souto *et al.*, 2004; Jenning *et al.*, 2000). This controlled release mechanism prevents a sudden intake of high concentration of irritating compounds into skin and also improve therapeutic efficacy of certain drugs such as anaesthetic or antimicrobial agents (Kheradmandnia *et al.*, 2010; Leng *et al.*, 2012).

Lipid nanoparticles have high potential to be commercial as the cosmetic and pharmaceutical products because it is easily mixed into the conventional formulations like gels or creams. Ketoconazole loaded SLN was successfully formulated into hydrogel and performed effectively in treatment of candidiasis (Ramasamy *et al.*, 2012). Flurbiprofen loaded lipid nanoparticles gels also showed a sustained anti-inflammatory activity for longer period of time (Bhaskar *et al.*, 2009). Nanolipid dispersion containing clotrimazole has been incorporated into base creams and showed longer release

character as compared to commercial creams (Souto & Müller, 2007). Indeed, some cosmetic products containing the SLN and NLC have been marketed as listed in Table 1.3.

Table 1.3: Examples of marketed lipid nanoparticles cosmetic products.

Product Name	Manufacturer	Date of Product Launched
Cutanova Cream Nano Repair Q10	Dr. Rimpler	10/ 2005
Nanolipid Q 10 CLR	Chemisches Laboratorium Dr. Kurt Richter, (CLR)	07/ 2006
NLC Deep Effect Repair Cream	Beate Johnen	12/ 2006
Regenerationscreme Intensive	Scholl	06/ 2007
SURMER Crème Contour Des Yeux	Isabelle Lancray	03/ 2008
NanoRemodelante Olivenöl Anti Falten Pflegekonzentrat	Dr. Theiss	02/ 2008

1.7 Objectives of Research

1. To prepare and characterize the physicochemical properties of stearic-oleic acid nanoparticles.
2. To investigate encapsulation efficiency of salicylic acid and lidocaine loaded stearic-oleic acid nanoparticles.
3. To study the load release kinetics of stearic-oleic acid nanoparticles in cream.

CHAPTER 2

MATERIALS AND
METHODOLOGY

2.1 Materials

Stearic acid with 95.0% purity and oleic acid with 99.0% purity were purchased from Sigma-Aldrich (St. Louis, USA) and Fluka (Buchs, Switzerland).

Tween series surfactants with 12 to 18 carbon hydrocarbon chain (Tween 20, Tween 40 and Tween 60) were obtained from Lasem Asia (Kuala Lumpur, Malaysia) and Sigma-Aldrich (St. Louis, USA). Salicylic acid (99.0%) and methanol (99.9%) were purchased from Merck (Darmstadt, Germany). Lidocaine with 98.0% purity and phosphate buffer saline (PBS) tablets (pH 7.4) were purchased from Sigma-Aldrich (St. Louis, USA). Salcare[®] SC91 based cream was obtained from BASF (Ludwigshafen, Germany).

All solutions and samples were prepared by using deionized water with a resistivity of $18.2 \Omega \text{ cm}^{-1}$, from a Barnstead Diamond Nanopure Water Purification unit coupled with a Barnstead Diamond[™] RO unit (Barnstead International, USA).

2.2 Preparation of SONs

SONs were prepared by melt-emulsification combined with ultrasonication method. The composition of SON without oleic acid that used in the early investigation of SONs preparation as listed in Table 2.1.

Table 2.1: Weight composition of SON preparation.

Composition	Weight (g)
Stearic acid	0.500
Tween 60	0.125
Water	5.000

The lipid phase, stearic acid was melted and dispersed in the pre-heated Tween 60 solution. This mixture was homogenized by using homogenizer (SilentCrusher M, Heidolph Instruments, Germany) at 75 °C to form emulsion. It was then further sonicated by using ultrasonic liquid processor model XL 2015 (USA). The nanoemulsion obtained was then poured into cold water to form nanoparticles.

Another series of SONs with different ratio of oleic acid were prepared for further investigations. In the preparation of SONs without the active ingredients, the lipid phases, stearic acid (0 wt% of oleic acid) or mixture of stearic acid and oleic acid with 10, 20, 30, 40 and 50 wt% oleic acid content, respectively, were prepared and melted at 75 °C. The molten lipid phases were mixed with pre-heated surfactant solutions. The mixtures were homogenized then further treated by ultrasonicator to form nanoemulsions. After that, the nanoemulsions were then poured into 20 mL of cold water (about 2 °C) to form SON nanoparticles. SON dispersions containing salicylic acid or lidocaine were prepared exactly the same manner by only adding salicylic acid or lidocaine into the lipid phases above. All SON dispersions were stored at 5 °C after preparation.

2.3 Particle Size and Polydispersity Index of SONs

The average particle size and polydispersity index of the SONs were measured by using ZetaSizer ZS (Malvern Instruments, UK) with a red Helium laser of wavelength $\lambda_0 = 633$ nm and at a backscattering angle of 7° . The average diameter of the particles was calculated by using the Stokes-Einstein equation with the assumptions that the particles are spherical and no interaction between them as shown in the following equation,

$$d = \frac{kT}{3\pi\eta D} \quad (1)$$

where d is diameter of the particles, the k is the Boltzmann's constant, T is the absolute temperature of the sample, η is the viscosity of the medium and D is the diffusion coefficient. In a monodisperse suspension, the correlation function of the scattered intensity $C(t')$ can be written as mono-exponential decay functions,

$$C(t') = A_c \left[1 + B \exp(-2\Gamma t') \right] \quad (2)$$

where A_c is the baseline of the correlation function, B is the intercept of the correlation function, Γ is the relaxation time which equal to $2Dq^2$, D is the diffusion coefficient, q is the scattering vector that which equal to $\frac{4\pi n'}{\lambda} \sin\left(\frac{\theta_s}{2}\right)$, n' is the refractive index of medium, θ_s is backscattering angle of measurement and t' is time delay between two intensities measurements. The average hydrodynamic diameter could be determined from the diffusion coefficient, D . The particle size distribution could be obtained from the equation (2) and the width of the size distribution compared to the median value is known as polydispersity index. The smaller value of polydispersity which closes to 0 indicated that the particle size of the sample is uniformly distributed.

Approximately, 0.5 ml of SON dispersion was diluted to 25 ml with deionized water and was equilibrated to room temperature for 10 min. A 1 cm path length clear quartz cuvette was used for the particle size measurement. All measurements were performed at a constant temperature of 25 °C. Mean particle size and polydispersity index were obtained from triplicate measurement of each diluted SON solution whereby each measurement consisting of 5 runs on the sample.

SON suspensions prepared were divided into three vials and kept at 5 °C, room temperature (28 °C) and 45 °C, respectively, for particles stability investigation. Measurements of the mean particle size of SON were performed throughout a period of 28 days.

2.4 Zeta Potential Measurement

Zeta potential is one of the characterizations that useful for the assessment of the physical stability of colloidal dispersions. The particle with larger value of zeta potential would have the higher degree of repulsion among the similarly charged particles in the dispersion. Generally, suspended particles are considered to be stable when absolute value of zeta potential is above 30 mV (Müller *et al.*, 2001). Electrophoretic mobility of SONs was measured by using ZetaSizer ZS (Malvern Instruments, UK) at 25 °C. By using parameters obtained and knowing the viscosity and dielectric constant of sample, the zeta potential value can be calculated by using Henry equation as shown in the following equation.

$$U_E = \frac{2\varepsilon\zeta f(ka)}{3\eta} \quad (3)$$

where U_E is electrophoretic mobility, ε is dielectric constant of medium, ζ is zeta potential, $f(ka)$ is Henry's function, η is viscosity of SON dispersion. Henry's function is related to Debye length (k) and reciprocal of Debye length (k^{-1}) provides the information of electric double layer thickness for a particle. Hence ka is deduced as ratio of the particle radius to the thickness of electric double layer ($a/(1/k)$). Smoluchowski approximation is applied for particle present in the polar solvent with $F(ka) = 1.5$ whereas Hückel approximation with $F(ka) = 1.0$ is used in the calculation for a non-polar solvent. SON dispersion was diluted 25 times with deionized water and was equilibrated to room temperature for 10 min. This measurement was carried out using disposable folded capillary cell. All measurements were performed at a constant temperature of 25 °C. An average value of zeta potential was obtained from triplicate measurement of each diluted SON solution whereby each measurement consisting of 12 runs on the sample.

2.5 Determination of Critical Micelle Concentration (CMC) of Surfactants

The effect of the surfactant hydrocarbon chain on the particle size of SONs could be explained by comparing the CMC of the surfactants. The CMC of Tween 20, Tween 40 and Tween 60 were determined by measuring the surface tension using the Du Nuoy ring method. A stock solution of 1 mmol L⁻¹ of Tween surfactant was prepared by dissolving appropriate amount of Tween surfactant in 100 ml deionized water. The stock solution was left to equilibrate at room temperature for overnight prior to any measurement.

A series of 50 ml solution with different concentration of Tween surfactants were prepared by diluting the surfactant stock solution with deionized water. The series of the surfactant solution prepared were let to equilibrate at room temperature for overnight prior to the surface tension measurement.

The sample solutions were filtered through a 25 mm diameter 0.2 µm pore size Minisart[®]NY nylon filter (Germany) prior to measurements. The CMC determinations were carried out *via* tensiometer balance from KRUSS with K 12 tensiometer processor *via* Du Nuoy ring method. The ring was initially cleaned and heated to red-hot with Bunsen burner before use. The samples were equilibrated at 30 °C for 10 min prior to measurements. All measurements were performed at a constant temperature of 30 °C throughout the experiments.

2.6 Transmission Electron Microscopy (TEM)

The morphological observations of SONs were obtained by using Energy Filtered TEM model LIBRA 120 equipped with an Olympus SIS-iTEM (version 5). Samples were diluted to around 0.8 wt% with deionized water and equilibrated at room temperature for 5 min. A piece of carbon-coated 400 mesh copper grid was held by using forceps and a drop of SON dispersion was placed onto the shining side of the carbon-coated 400 mesh copper grid. After 1 min, the excess dispersion droplet was then removed by using a piece of filter paper. It was then negatively stained with a drop of 2% phosphotungstic acid solution and left for 1 min. The grid was air-dried at room temperature for 30 min and then ready to be examined under TEM.

2.7 Differential Scanning Calorimetry (DSC) Analysis

DSC is one of the thermal analyses that usually used to obtained information on the physical and energetic properties of sample. DSC analysis has been widely used to determine the state and the degree of the crystallinity of lipid nanoparticles (Bunjes & Unruh, 2007). It allows the study of the melting and crystallization behavior of crystalline state in lipid nanoparticles. The loading capacity was generally associated with the degree of crystallinity because the crystalline state in lipid nanoparticles determined the accommodation spaces of payload ingredients. The degree of crystallinity is defined as the percentage of the crystalline state in the lipid matrix that has recrystallized during the cooling process in the preparation of lipid nanoparticles. The degree of crystallinity of SONs was determined by calculating the ratio of SON enthalpy to stearic acid enthalpy as shown by the following equation:

$$CD = \left(\frac{H_{SON}}{H_{SA}} \right) \times 100\% \quad (4)$$

where CD is degree of crystallinity of SON, H_{SON} is enthalpy of SON and H_{SA} is the enthalpy of pure stearic acid, respectively. Thermal behaviours of SONs were analysed by using Tzero™ DSC Q 20 (TA Instruments, USA). Approximately, 1 ml of SON dispersions was dried in a desiccator for 24 hours prior to DSC analysis. About 6 mg of air-dried SON sample was weighed into 40 μ L aluminium sample pan. An empty sample pan was used as a reference. The heating run was performed from 35 $^{\circ}$ C to 80 $^{\circ}$ C with the heating rate of 5 $^{\circ}$ C min^{-1} by continuously flushing the nitrogen gas at the rate of 20 mL min^{-1} . The DSC parameters such as melting point, onset temperature, melting enthalpy were analysed by using TA Universal Analysis software (TA Instruments, USA).

2.8 Preparation of Standard Concentration Curve of Salicylic Acid for UV-Visible Spectrophotometry Measurement

A stock solution of 100 mg L^{-1} of salicylic acid solution was prepared by dissolving 10 mg salicylic acid in 50 mL deionized water and then made up to 100 mL in a volumetric flask. After that, a series of salicylic acid solution with the concentration of 2.5 mg L^{-1} , 5 mg L^{-1} , 10 mg L^{-1} , 20 mg L^{-1} and 40 mg L^{-1} were prepared by diluting the salicylic acid stock solution. The prepared salicylic acid solutions were measured spectrophotometrically by using Varian UV-visible spectrophotometer model Cary 50 (Agilent technologies, US) at the wavelength of 297 nm and the standard concentration curve of salicylic acid was plotted.

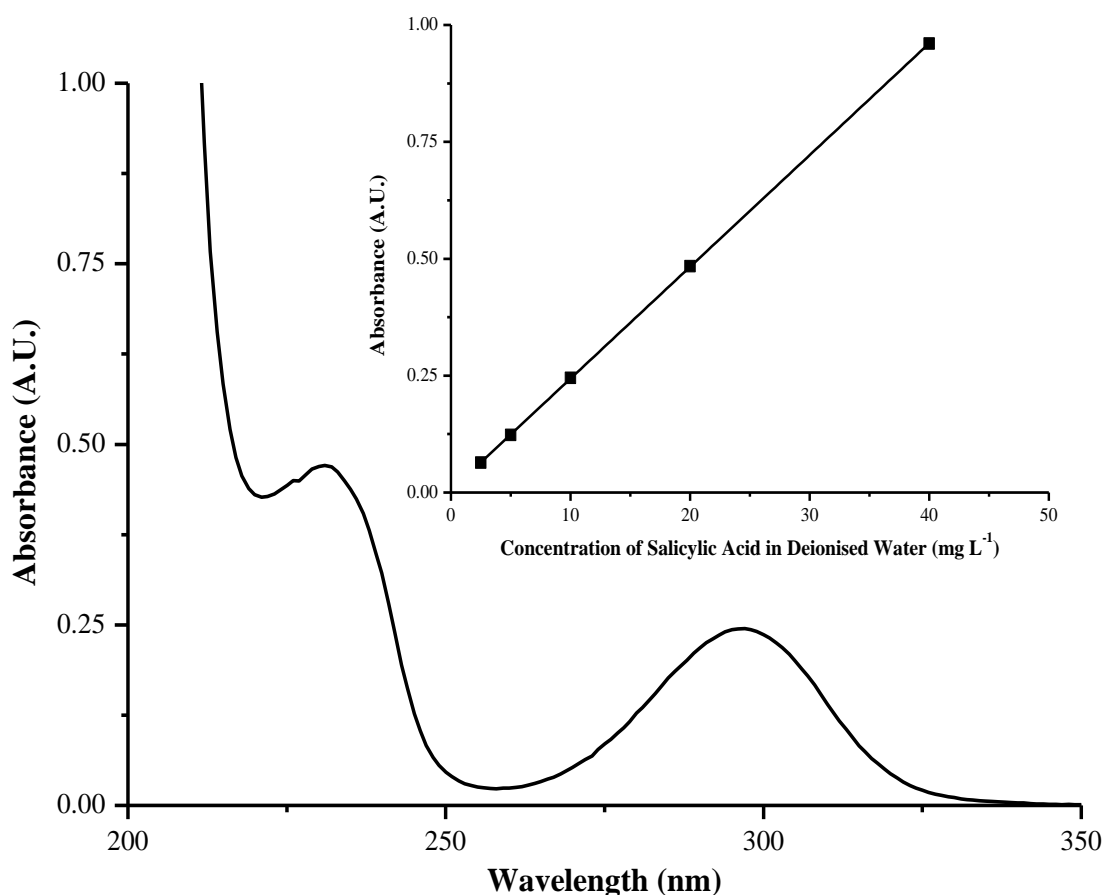


Figure 2.1: UV-Vis absorption spectrum and standard concentration curve (small) of salicylic acid in deionized water at 25 °C.

2.9 Preparation of Standard Concentration Curve of Lidocaine for UV-Visible Spectrophotometry Measurement

A stock solution of 300 mg L^{-1} of lidocaine solution was prepared by dissolving 30 mg lidocaine in 50 mL deionized water and then made up to 100 mL in a volumetric flask. The lidocaine stock solution was sonicated to ensure the lidocaine crystal was totally dissolved in the deionised water. A series of lidocaine solutions with the concentration of 10 mg L^{-1} , 25 mg L^{-1} , 50 mg L^{-1} , 100 mg L^{-1} , 150 mg L^{-1} and 250 mg L^{-1} were diluted from the stock solution with deionized water. The prepared lidocaine solutions were measured spectrophotometrically at the wavelength of 263 nm. Then, the standard concentration curve of lidocaine was plotted with the data obtained.

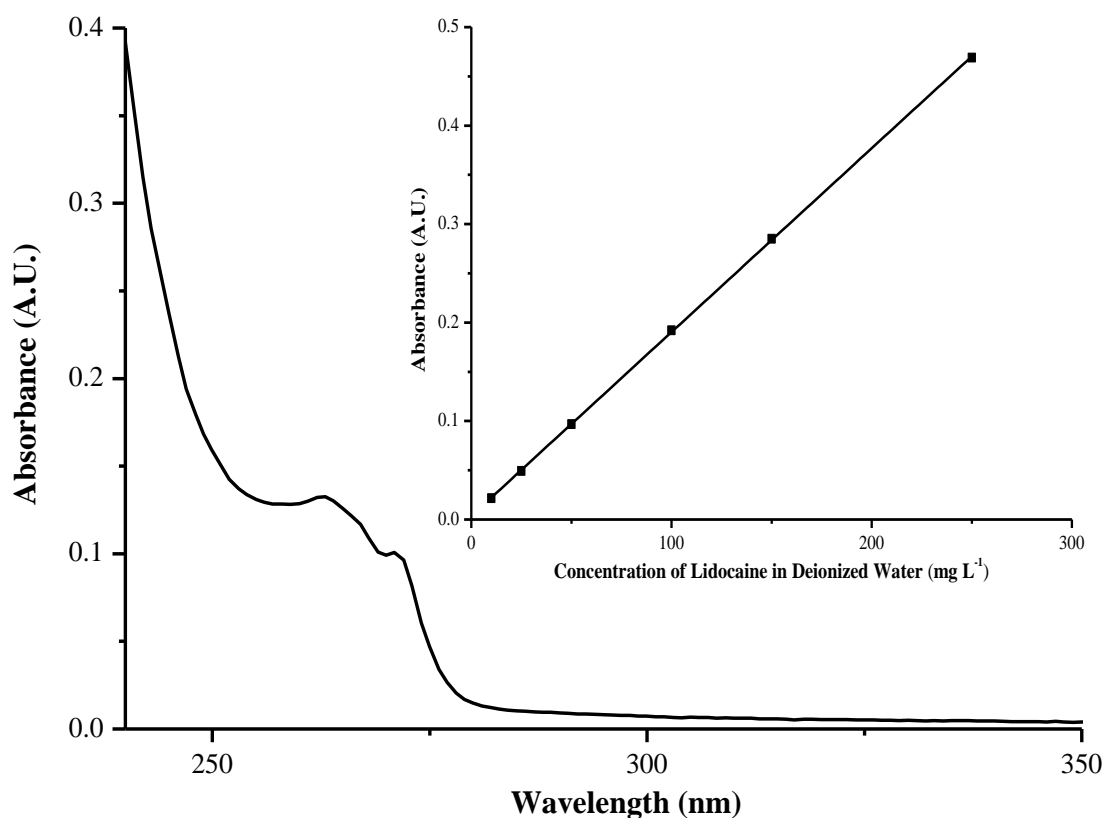


Figure 2.2: UV-Vis absorption spectrum and standard concentration curve (small) of lidocaine in deionized water at 25 °C.

2.10 Encapsulation Efficiency of SONs

Encapsulation efficiency of salicylic acid or lidocaine loaded SON was determined using centrifugal ultrafiltration method (Figure 2.3). SON dispersion was placed into the upper chamber of centrifugal filter tubes with 50000 Da molecular weight cut-off (Vivaspin 6, Sartorius Stedim Biotech, Germany) and centrifuged for 30 min at 8000 rpm. Then, the concentration of free salicylic acid or lidocaine in the supernatant was determined spectrophotometrically by using UV-visible spectrophotometer with 1 cm path length clear quartz cuvette at a constant temperature of 25 °C which thermostatically controlled by a *Peltier* unit and cooled with water circulator. The amount of salicylic acid or lidocaine in each sample was determined from the standard concentration curves (Figure 2.1 and 2.2). Encapsulation efficiency was calculated by the following equation:

$$EE = \left(\frac{W_T - W_F}{W_T} \right) \times 100\% \quad (4)$$

where EE is encapsulation efficiency of SON, W_T is the weight of salicylic acid or lidocaine added during preparation and W_F is the weight of free salicylic acid or lidocaine in the supernatant, respectively.

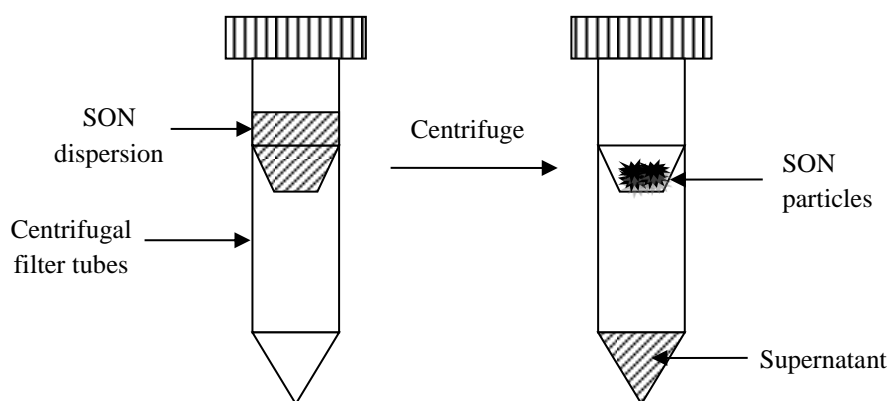


Figure 2.3: Schematic diagram of centrifugal ultrafiltration by using Vivaspin.

2.11 Sample Preparation for *In Vitro* Release Evaluation

Eight different samples were prepared for the *in vitro* release evaluation. The first four different samples of salicylic acid solution, salicylic acid cream, salicylic acid loaded SON and salicylic acid loaded SON incorporated into cream were denoted as Sample A, B, C and D. Sample A was prepared by dissolving salicylic acid in deionised water. Sample B was prepared by homogenizing the salicylic acid solution and Salcare[®] SC91 base cream obtained from BASF, a raw material that consisted of 8% anionic acrylic copolymer dispersed in a 5-8% of medical grade white oil. Sample C is the optimized salicylic acid loaded SON dispersion and this SON dispersion was further formulated into Salcare[®] SC91 base cream at the homogenization rate of 5000 rpm for 5 min to prepare Sample D.

For the samples which containing lidocaine, these sample were prepared same manner as described above with replacing the salicylic acid to lidocaine. Lidocaine solution, lidocaine cream, lidocaine loaded SON and lidocaine loaded SON incorporated into cream were denoted as Sample E, F, G and H.

2.12 Preparation of Standard Concentration Curve of Salicylic Acid for *In Vitro* Release Study

A stock solution of 50 mg L^{-1} of salicylic acid solution was prepared by dissolving 5 mg salicylic acid in 50 mL 10 mM PBS (pH 7.4) and then made up to 100 mL in a volumetric flask. After that, a series of salicylic acid solution with the concentration of 1.563 mg L^{-1} , 3.125 mg L^{-1} , 6.25 mg L^{-1} , 12.5 mg L^{-1} and 25 mg L^{-1} were prepared by diluting the salicylic acid stock solution. The prepared salicylic acid solutions were measured spectrophotometrically at the wavelength of 297 nm and the standard concentration curve of salicylic acid was plotted.

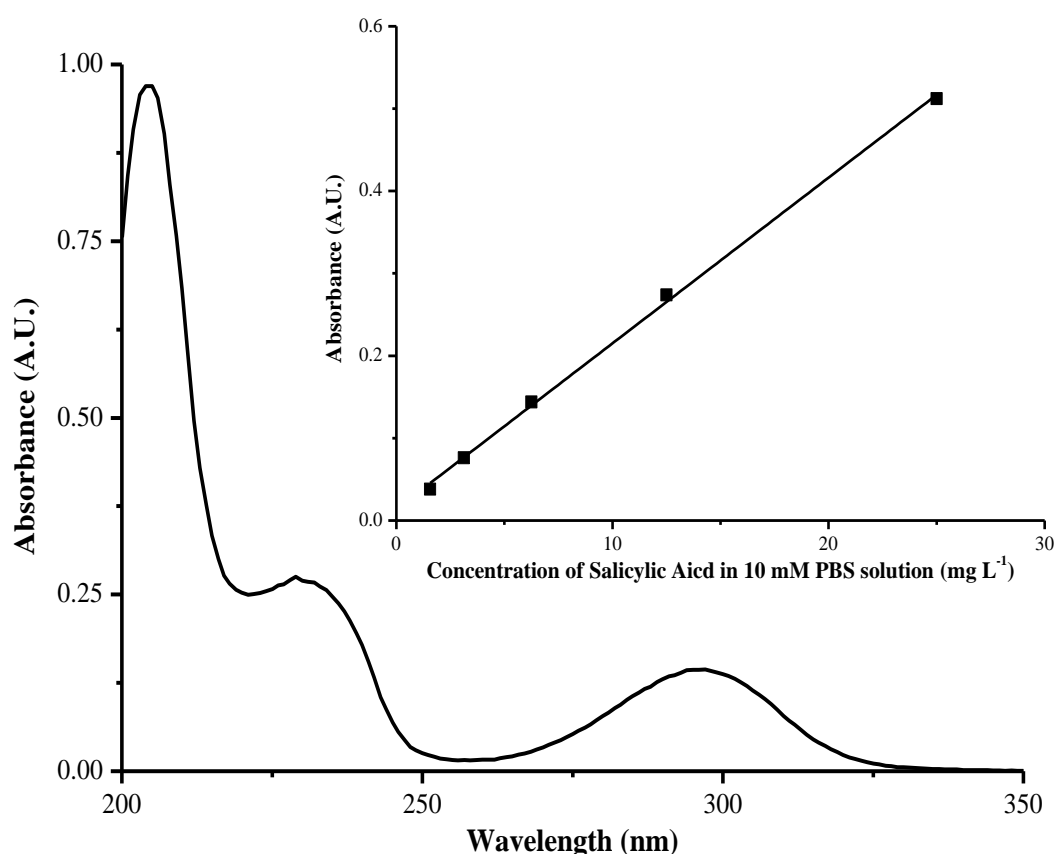


Figure 2.4: UV-Vis absorption spectrum and standard concentration curve (small) of salicylic acid in 10 mM PBS solution at 25 °C.

2.13 Preparation of Standard Concentration Curve of Lidocaine for *In Vitro* Release Study

A stock solution of 50 mg L^{-1} of lidocaine solution was prepared by dissolving 5 mg lidocaine in 50 mL 10 mM PBS (pH 7.4) and then made up to 100 mL in a volumetric flask. After that, a series of lidocaine solution with the concentration of 1.25 mg L^{-1} , 2.5 mg L^{-1} , 5 mg L^{-1} , 7.5 mg L^{-1} , 10 mg L^{-1} and 15 mg L^{-1} were prepared by diluting the lidocaine stock solution. The prepared lidocaine solutions were measured spectrophotometrically at the wavelength of 263 nm and the standard concentration curve of lidocaine was plotted.

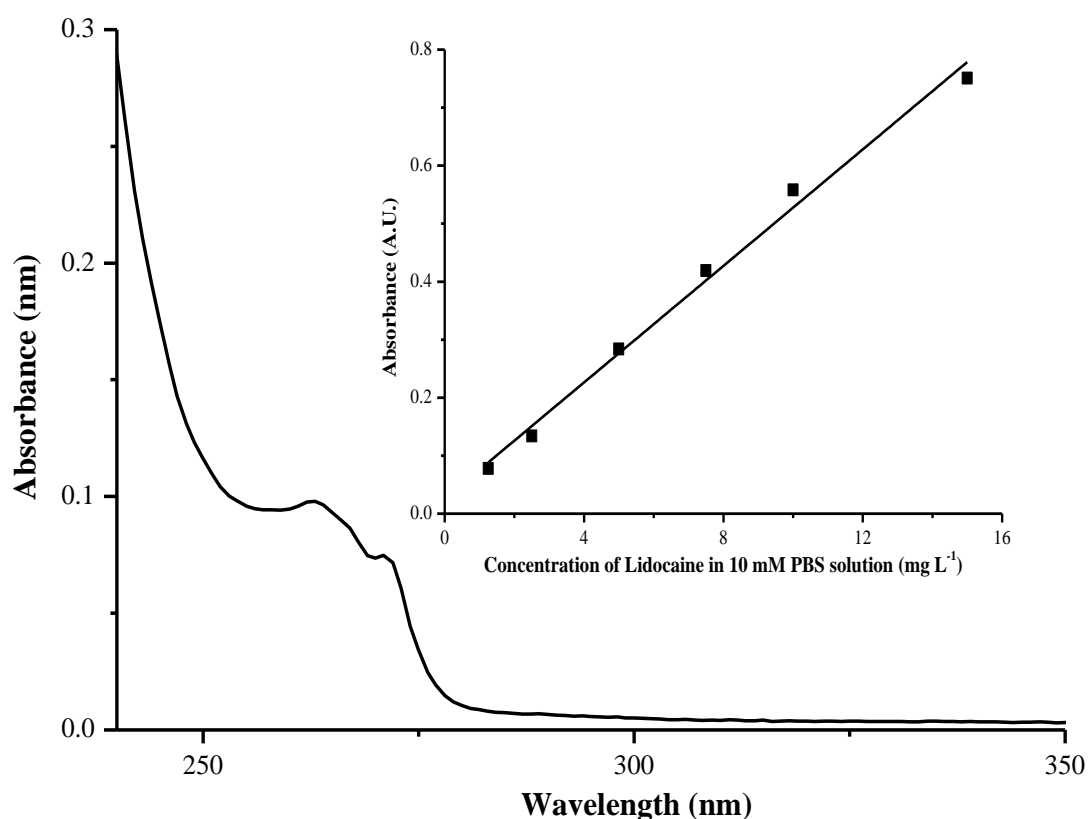


Figure 2.5: UV-Vis absorption spectrum and standard concentration curve (small) of lidocaine in 10 mM PBS solution at 25 °C.

2.14 *In Vitro* Release Evaluation

In vitro Franz diffusion technique was one of the methods for evaluation the *in vitro* release rate of active ingredient and/or drug from the samples. In this study, the Automated Franz Diffusion Cell System from Hanson Research was employed in the drug release experiment. The Franz Diffusion Cell System which employs six vertical, water jacketed Franz diffusion cells with helix spring stirrer which ensure the homogeneity of the sample throughout the experiment. The six cells were connector to a bath circulator (PolyScience, USA) that was used to maintain constant temperature throughout the experiment. The syringe pumps were used to withdraw the sample and replace it with fresh receiving medium. The last component of the system is the sample collector with six nozzles which delivers the sample from the Franz diffusion cells to the programmed position and loads it into the sample vials.

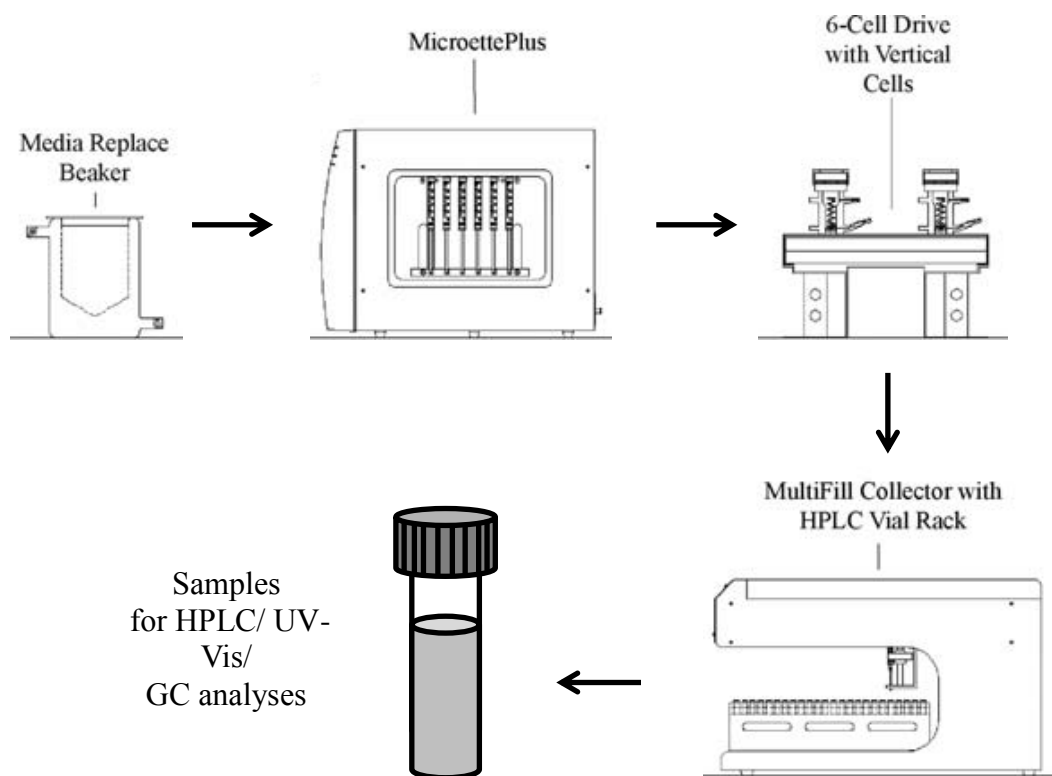


Figure 2.6: Schematic diagram of Automated Franz Diffusion Cell System employed in this experiment.

The *in vitro* drug releases of the four different samples were evaluated by using Franz diffusion cells (Figure 2.7) with 0.636 cm² of effective diffusion area and 4 mL of diffusate chamber volume. The diffusate compartments were filled with a 10 mM PBS pH 7.4, stirred at 400 rpm and thermostated at 37±1 °C during all the experiments. Regenerated cellulose membranes with a 5000 Da molecular weight cut-off were used in these experiments. Pre-treatment of the membranes by soaking in the receiving medium were performed for 1 hour before mounted to the Franz diffusion cells. The regenerated cellulose membranes were sandwiched between the retentate and diffusate chamber. Approximately 1 g of each sample (1 g L⁻¹) was placed on the membrane surface in the retentate chamber. Each experiment was performed by using six different retentate chambers for 24 hours. At predetermined intervals, samples were withdrawn and replaced with fresh receiving medium. These samples were spectrophotometrically analysed in order to obtain the concentration of salicylic acid or lidocaine as describe in Section 2.9. The amount of salicylic acid or lidocaine in each sample was determined from the standard concentration curves (Figure 2.4 and 2.5). Each data point was as the average of six measurements.

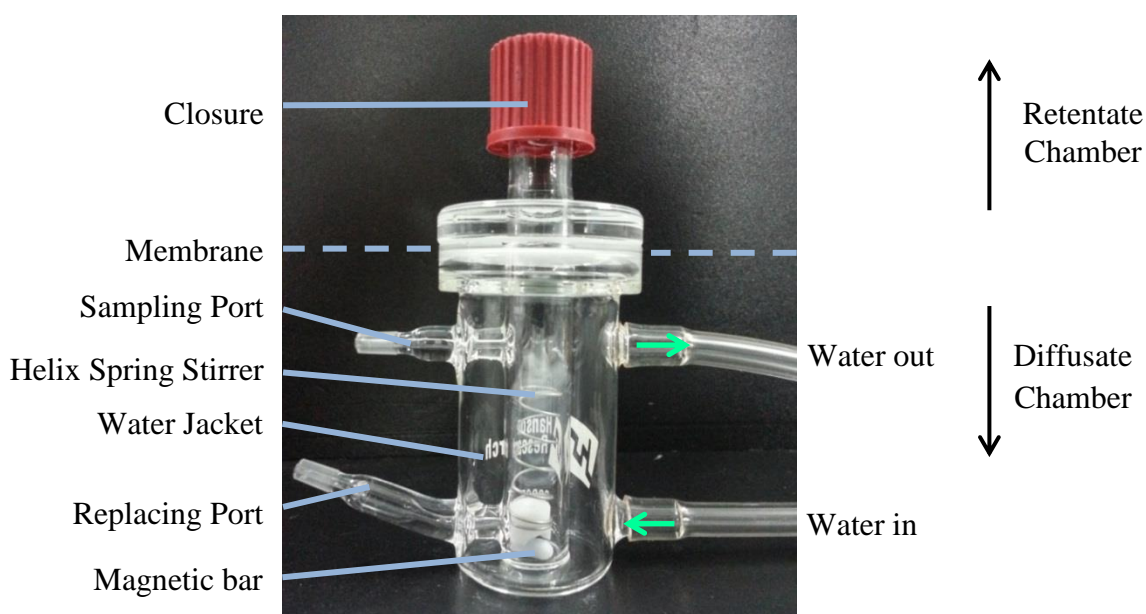


Figure 2.7: Photograph of Franz Diffusion Cell.

CHAPTER 3

RESULTS AND DISCUSSIONS

3.1 Particle size Analysis

3.1.1 Effect of Homogenization Time on Mean Particle Size of SONs

One of the objectives in this study is to prepare a stable SON dispersion with desired particle size (less than 500 nm). The size and physical stability of SON depends on the preparation parameters (time of homogenization, shear rate and sonication time), compositions (fatty acid compositions, concentration of surfactant and ingredients) and the storage temperature. A series of experiments were carried out to achieve this objective.

Formation of emulsion is a non-spontaneous process and usually required energy input and sufficient time to disperse one liquid to another liquid phase. In this experiment, the effect of homogenization time on particle size was investigated. All SONs were prepared using the same parameters (homogenized at 15000 rpm then sonicated for 60 s) with varies the homogenization time from 150 s to 600 s. It was observed that the mean particle size of SONs greatly reduced about 21% with increased homogenization time from 150 s to 300 s at the same homogenization rate (Table 3.1).

Meanwhile, the SON which homogenized for 300 s was lower polydispersity index than the SON which only homogenized for 150s. This is because emulsion droplets experienced the shear forces which overcome its interfacial force and caused the breakup of emulsion droplets during homogenization process. By applying the same shear force, sufficient homogenization time is required for the deformation and disruption of larger emulsion droplets into smaller ones (McClements, 1998). However, the mean particle size of SON only reduced about 4% with increased the homogenization time from 300 s to 600 s (Table 3.1). This result showed that homogenization for 300 s is enough time for emulsion to achieve the desired size.

Table 3.1: Effect of homogenization time on mean particle size and polydispersity index of SONs at 25 °C.

Homogenization Time (s)	Mean Particle Size (nm)	Polydispersity Index
150	280 ± 4	0.34 ± 0.02
300	221 ± 2	0.16 ± 0.02
600	212 ± 3	0.14 ± 0.02

3.1.2 Effect of Homogenization Speed on Mean Particle Size of SONs

When both oil and water are mixed, two layers of liquids will eventually be obtained. Usually mechanical agitation is applied to mix oil and water in order to form emulsion.

By maintaining other variables constant, further investigation on the particle size of SONs was carried out by changing the homogenization speed. There is about 14% reduction in mean particle size of SON that homogenized at 10000 rpm as compare to 5000 rpm (Table 3.2). The average particle size of SON is further reduced to about 15% when the homogenization speed was increased up to 15000 rpm. However, it is only slightly reduced in mean particle size (about 6%) when homogenization speed reached 20000 rpm.

A more monodisperse SON dispersion was obtained with increasing homogenization rate from 5000 rpm up to 15000 rpm, further increased in homogenization rpm speed does not significantly reduced the polydispersity of nanoparticles. This is because droplets experience a shearing force which causing it rotate, circulate and become elongated during homogenization (McClements, 1998). At higher homogenization rate, a greater external force was exerted on to the emulsion, overcomes the interfacial force and consequently caused the elongated droplets broken up into a number of smaller droplets (Tadros, 2006). However, homogenization speed

was further increased up to 20000 rpm only slightly reduced the mean particle size about 10 nm which indicate the 15000 rpm is sufficient and used here forth.

Table 3.2: Effect of homogenization speed on mean particle size and polydispersity index of SONs at 25 °C.

Homogenization Speed (rpm)	Mean Particle Size (nm)	Polydispersity Index
5000	287 ±4	0.24 ±0.01
10000	247 ±3	0.23 ±0.02
15000	211 ±2	0.16 ±0.02
20000	199 ±3	0.12 ±0.02

3.1.3 Effect of Sonication Time on Mean Particle Size of SONs

Ultrasonication process generally contributes to a mechanism of cavitation which the ultrasound waves resulting a mechanical depressions and compressions and generating cavitation and subsequently provides sufficient energy to increase the surface area of the emulsion hence formation of nanoemulsion (Jafari *et al.*, 2006).

The effect of sonication time (0 s, 30 s, 60 s and 120 s) on particle size of SON was investigated. A significantly reduction in mean particle size from 324 nm to 241 nm (about 26%) was observed (Table 3.3) when sonication applied to the pre-homogenized emulsion for 30 s. Smaller particles (200 nm) with lower polydispersity was obtained by further increasing the time of sonication up to 120 s. This may be due to sufficient time is need for the repetition of cavitation activities to generate smaller droplets of emulsion.

Although applying sonication during preparation of SON could reduce the particle size, however prolong high energy input may release the titanium oxide from the microtip of ultrasound processor. Therefore, the maximum time for sonication process was limited to 120 s to avoid contamination on sample.

Table 3.3: Effect of sonication time on mean particle size and polydispersity index of SONs at 25 °C.

Sonication Time (s)	Mean Particle Size (nm)	Polydispersity Index
0	324 ± 5	0.23 ± 0.02
30	241 ± 5	0.17 ± 0.03
60	211 ± 2	0.16 ± 0.02
120	200 ± 3	0.12 ± 0.02

3.1.4 Effect of Lipid Content on Mean Particle Size of SONs

Lipid content is one of the important parameter in the preparation of SON. Optimum lipid content need to be determine because higher lipid content could incorporate higher amount of active ingredient and the same time SON particles need to maintain in certain size range. The effect of lipid content in SON dispersion on average size of particles was investigated. For this investigation, the ratio of lipid to surfactant was kept constant at 4:1 and the weight of deionised water still kept at 5 g. The total amount of lipid content were increased from 1.25 wt%, 2.5 wt%, 5.0 wt%, 10 wt% and 15 wt% in the formulation of SON dispersions.

The average particle size of SONs increased linearly with increasing the lipid content. The mean particle size of SON dispersion increased about 60% by increasing the lipid content from 1.25 wt% to 15 wt% (Figure 3.1). At the same time, its polydispersity index also increased from about 0.1 to 0.3 with increasing the lipid content in the formulations. This may be due to the increased in the overall viscosity with an increase in the lipid content, subsequently decrease the effectiveness of homogenization and hence larger particles and broader particle size distributions were obtained (Mehnert & Mäder, 2012).

In this study, unloaded SON with mean particle size less than 250 nm is preferable because assuming of active ingredients will further enlarge the mean particle size of SON. Therefore, SON with 2.5 wt% lipid content, which gives an average particle size around 230 nm, was chosen throughout these experiments.

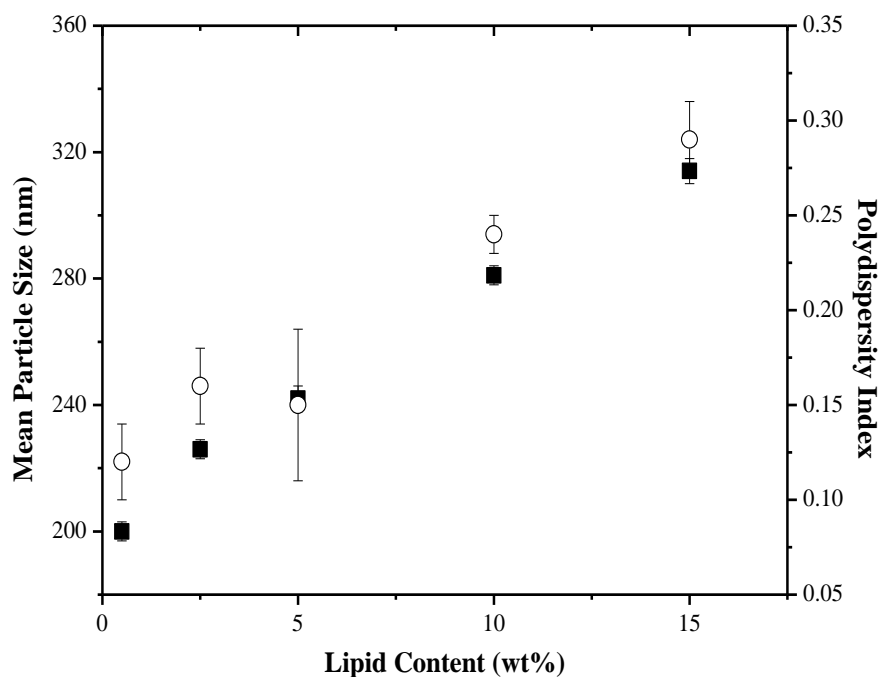


Figure 3.1: Plot of mean particle size (■) and polydispersity index (○) of SONs as function of lipid content at 25 °C.

3.1.5 Effect of Oleic Acid Composition on Mean Particle Size of SONs

SLNs are lipid nanoparticles that composed of single or mixed solid lipids. Its inherence crystalline structure has known to give several advantages such as low loading capacity and expulsion of drugs and/or active ingredients during storage. To overcome these limitations, liquid oils were incorporated into lipid nanoparticles to effectively improve the loading efficiency of drugs and/or active compounds. However, the physicochemical properties of lipid nanoparticles will be difference caused by the incorporation of oil. In this study, oleic acid was introduced into the stearic acid matrix during the preparation of SON.

A series of SON dispersions were prepared by mixing different amount of oleic acid from 0 wt% to 50 wt%. It was observed that the mean particle size of SON depended on the amount of oleic acid in the mixture. The average particle size of unloaded SONs increased from 194 nm to 255 nm with increasing oleic acid amount up to 30 wt%, while it decreased about 13% when the oleic acid composition achieved up to 50 wt% (Table 3.4). These observations indicated that the excipients' mean particle sizes directly affected by the amount of oleic acid in the mixture. This may be due to the participation of oleic acid in the formation of nanoparticles (Woo *et al.*, 2014). However, the decrease in size of the particles with higher amount of oleic acid (>40 wt%) may be due to the incompatible mixing between stearic acid and oleic acid.

Table 3.4: Mean particle size and polydispersity index of freshly prepared SONs with different oleic acid compositions at 25 °C.

Oleic Acid Content (wt%)	Mean Particle Size (nm)	Polydispersity Index
0	194 ± 2	0.19 ± 0.01
10	221 ± 4	0.21 ± 0.02
20	246 ± 3	0.31 ± 0.03
30	255 ± 3	0.37 ± 0.02
40	229 ± 4	0.37 ± 0.01
50	223 ± 4	0.36 ± 0.02

3.1.6 Effect of Surfactant Chain Length on the Size of SON Particles

Besides the physical nature of fatty acid in the mixture, the overall cohesive energy in between different mixture of composition is also expected to influence SON properties. Different in hydrocarbon chain length of surfactant directly affected the hydrophilic-lipophilic balance (HLB) and CMC values which closely associated to the lowering interfacial free energy and formation of emulsion droplets (Franzetti *et al.*, 2010).

A series of Tween surfactants with different hydrocarbon chain length were used in preparation of SONs. Tween 20, 40 and 60 were Tween type surfactants with 12, 16 and 18 hydrocarbon chain length, respectively. The SONs stabilized by the Tween 60 having the smallest particle size, whereas larger particles obtained with the used of shortest hydrocarbon chain of surfactants. From the data obtained (Figure 3.2), it is clearly showed that the average particle size of SON is inversely proportional to the hydrocarbon chain length of surfactants. The mean particle size of SONs reduced about 40 nm with increasing the hydrocarbon chain length of Tween surfactants.

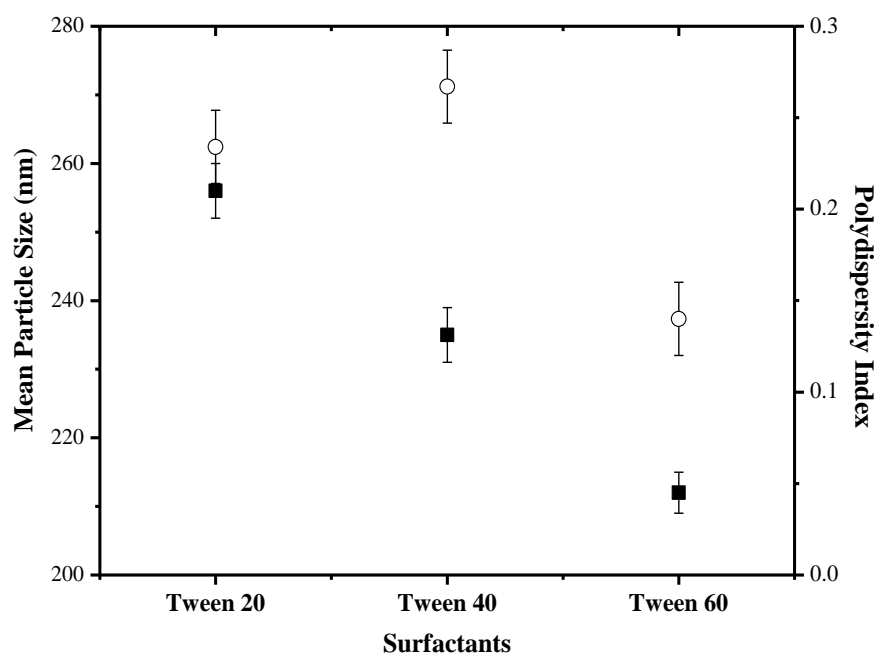


Figure 3.2: Plot of mean particle size (■) and polydispersity index (○) of SONs as function of surfactant chain length at 25 °C.

HLB described the hydrophilic or lipophilic property of a surfactant based on its polar or non-polar moieties of the surfactant molecule. HLB value of Tween 20, 40 and 60 is 16.7, 15.6 and 14.9, respectively (Umbreit & Strominger, 1973). Surfactant with a high HLB value usually form o/w emulsion and vice versa. Tween 60 has lower HLB value than Tween 20 and 40 indicates that it is more lipophilic which is energetically unfavourable in water and more likely to self-assemble into aggregates at lower concentration in order to minimize the hydrophobic effect.

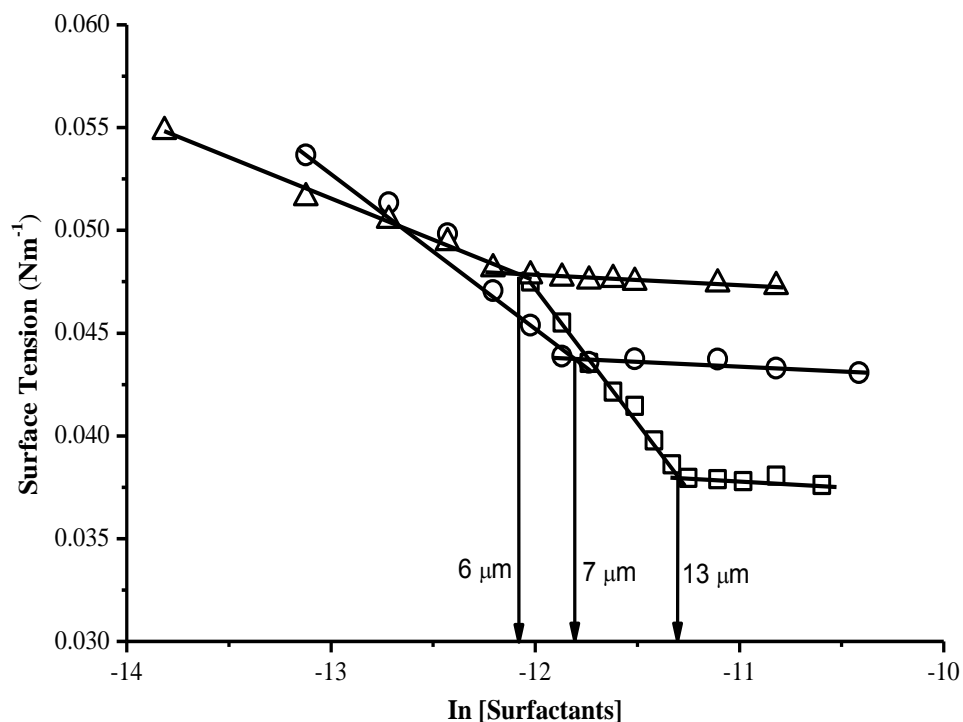


Figure 3.3: Plot of surface tension as a function of $\ln[\text{surfactants}]$ of Tween 20 (\square), Tween 40 (\circ) and Tween 60 (Δ) at 25°C.

Figure 3.3 shows that the size of SONs was associated to the CMC of surfactants. It was found that the CMC decreased with increasing hydrocarbon chain (Figure 3.3). The CMC values that obtained from this experiment were about 13 μM , 7 μM and 6 μM for Tween 20, Tween 40 and Tween 60, respectively. The surfactant with longer hydrocarbon tail has higher hydrophobic interaction between the surfactant monomers and able to form micelle at lower concentration. Therefore, it is able to form smaller emulsion droplets as compared to other Tween type surfactants with shorter hydrocarbon chain for the same surfactant concentration. In this case, Tween 60 was the best candidate among the Tween type surfactants for the preparation of SON since it could form the smallest particles.

3.1.7 Effect of Surfactant Concentration on the Size of SON Particles

The presence of surfactant plays an important role in the formulation of SON to assist in the emulsification process and helps stabilization of lipid nanoparticles by adsorbing onto the surface of particle and thereby sterically stabilizing the particle from aggregation.

It has been shown in the previous section that Tween 60 nonionic surfactant was used because it has shown to produce smaller particles among the surfactants studied. A series of different amounts of Tween 60 were used to investigate the effect of surfactant concentration on the particle size of SONs. It was observed that the particle size of SON with 2% w/v of surfactant was reduced to about 60% smaller as compared to the SON with 0.25% w/v of surfactant (Figure 3.4).

On the other hand, SON dispersion was observed to be less turbid at higher concentration. The appearance of SONs changed from whitish to bluish colour with increasing the amount of surfactant (Figure 3.5). This phenomenon indicated that the changes in larger size to smaller size of SON particles.

It was reported that higher concentration of surfactant solution is more effectively to lower the interfacial free energy between oil and water (Riangjanapatee & Okonogi, 2012). Considering the data obtained from this experiment, it could be assumed that the small particle size of the SON obtained from the higher amount of Tween 60 was as a consequence of decreasing interfacial free energy between the two immiscible lipid and aqueous phases during the emulsion forming process.

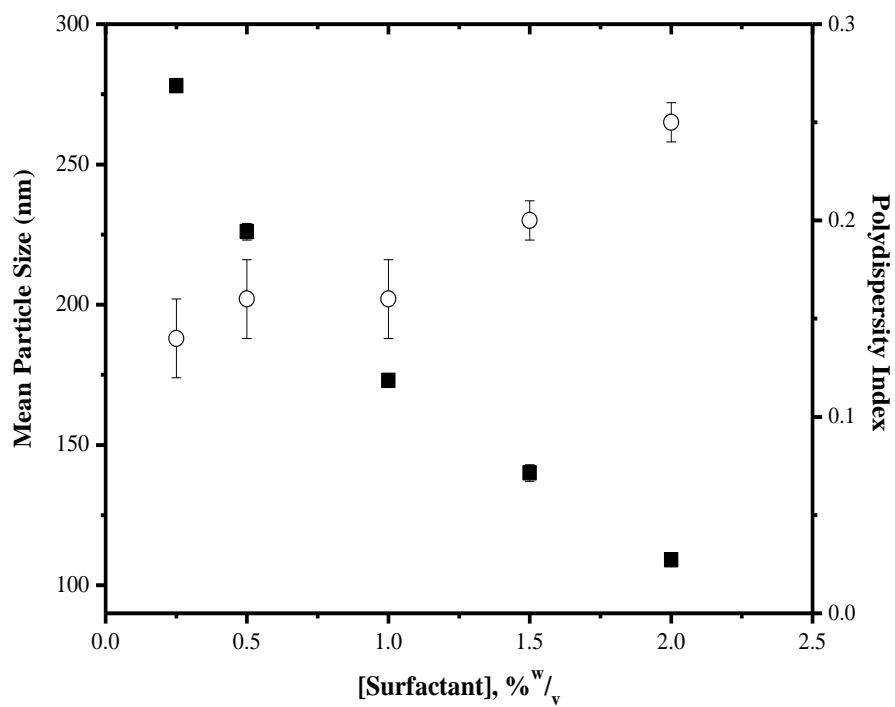


Figure 3.4: Plot of mean particle size (■) and polydispersity index (○) of SONs as function of surfactant concentration (% w/v) at 25 °C.

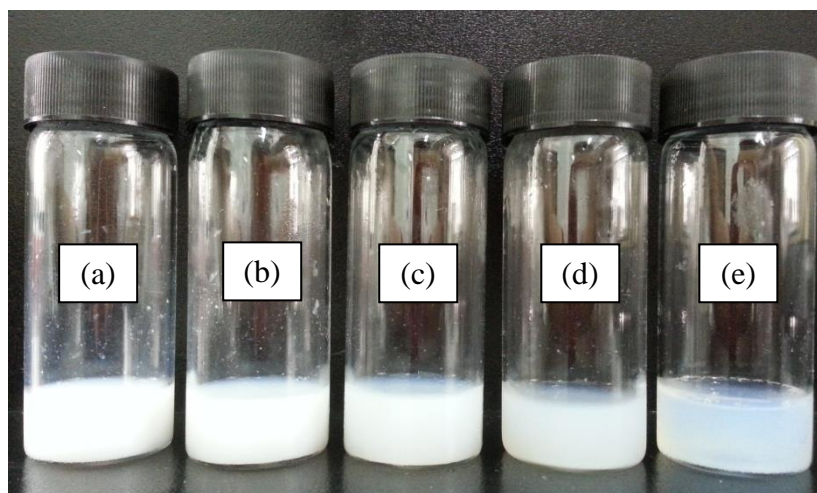


Figure 3.5: SON dispersions stabilized by (a) 0.25% w/v, (b) 0.50% w/v, (c) 1.00% w/v, (d) 1.50% w/v and (e) 2.00% w/v of Tween 60.

3.1.8 Effect of Active Compounds in the Composition on the Particle Size of SONs

As a carrier system, SONs are able to carry active ingredients or drugs by encapsulating them into its matrix. In this study, two active ingredients namely salicylic acid and lidocaine were chosen for the encapsulation into lipid matrix and their effect on mean particle size of SONs with 30 wt% oleic acid was investigated.

A dramatically increased about 27% in the mean particle sizes of SON with 30 wt% oleic acid loaded with 5 mg of salicylic acid was observed as compared to its unloaded SONs (Table 3.5). The size of SONs was further increased 378 nm when amount of salicylic acid added up to 30 mg. The substantially increased in mean particle size was indicated that the salicylic acid participation in the formation of SON nanoparticles (Woo *et al.*, 2014). Similar results for incorporation of other active ingredients or drugs into lipid nanoparticles have also been reported (Chattopadhyay *et al.*, 2007; Das *et al.*, 2012).

At the same time, an interesting finding for SONs with 30 wt% oleic acid containing lidocaine was observed. Besides a similar increasing trend in size of SONs with lidocaine was observed, it is also found that smaller particles were obtained as compared to SONs with salicylic acid (Table 3.5). This is may be due to the lidocaine is more compatible with the SON matrix as compared to salicylic acid.

Table 3.5: Mean particle size and polydispersity index of freshly prepared salicylic acid or lidocaine loaded SON with 30 wt% oleic acid at 25 °C.

Amount of Active Ingredients (mg)	Salicylic Acid loaded SONs		Lidocaine loaded SONs	
	Mean Particle Size (nm)	Polydispersity Index	Mean Particle Size (nm)	Polydispersity Index
	0	255 ± 2	0.37 ± 0.02	255 ± 2
5	324 ± 2	0.36 ± 0.02	270 ± 4	0.33 ± 0.04
10	332 ± 3	0.37 ± 0.02	284 ± 5	0.35 ± 0.02
20	351 ± 4	0.36 ± 0.02	297 ± 3	0.37 ± 0.02
30	378 ± 3	0.30 ± 0.04	321 ± 3	0.23 ± 0.02

3.2 Accelerated Stability Studies of SON

3.2.1 Effect of Surfactant Concentration

Nanoparticle stability was the major concern as the suspension stability exerted a great impact on the suspension ability to be practically functional and the capability to resist destabilization throughout the lifetime of the product. The destabilisation of lipid nanoparticles could be visually determined by observing the physically changes such as present of large particles, sedimentation or colour change from clear to turbid. Besides that, it is also could quantitatively determine by measuring the change in particle size and surface charge for certain period.

A series of SON with different amount of surfactant were prepared and stored at 45 °C for accelerated stability study. Any change in particle size can be monitored from particle size measurement carried out at each day (Figure 3.6). SONs with Tween 60 concentration up to 0.5% w/v in formulation only marginally increased about 15 nm in particle size. However, SONs with 1.0% w/v of Tween 60 showed gradually increased in particle size about 20% and significantly increased about 70% and 220% for 1.5% w/v and 2.0% w/v, respectively. This result suggested that the Tween 60 concentration should not exceed 1.0% w/v in the SON formulation.

The zeta potential values of SONs were gradually reduced as the concentrations of Tween 60 was increased (Table 3.6). This is may be due to the adsorption of Tween 60 onto the surface of lipid nanoparticles and hindered the carboxyl functional group of fatty acid which contributing the negative surface charge and subsequently reduced the zeta potential of lipid nanoparticle.

Although smaller particles could be obtained by increasing the surfactant concentration, it may not suitable to be used in preparation of SONs due to other factors such as size, polydispersity and surface charged that directly influence its stability also

need to take into consideration. Therefore, the concentration of Tween 60 in SON formulation in this case was kept constant at 0.5%^{w/v} for the further experiments.

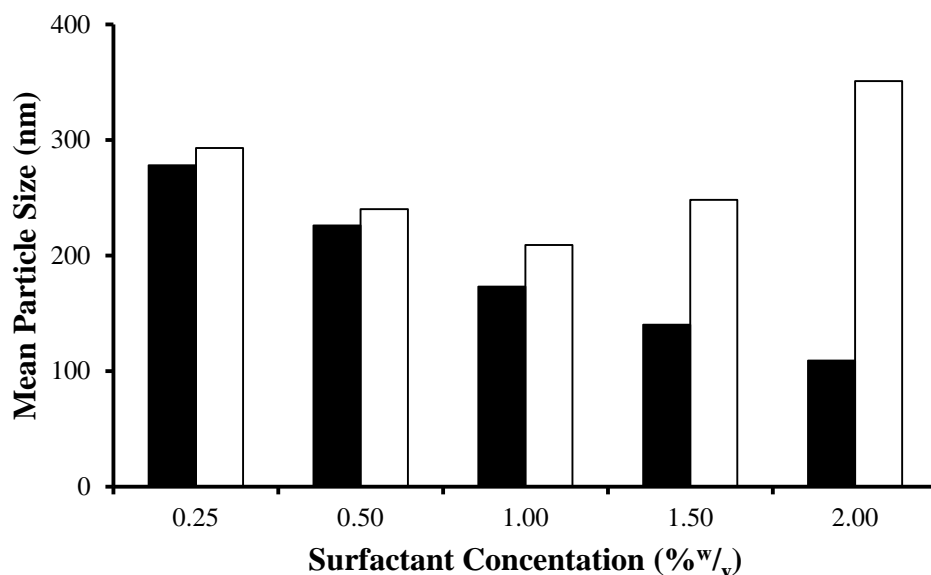


Figure 3.6: Accelerated stability of SON dispersions with different surfactant concentration in formulation at 45°C for 1 day (■) and 4 days (□) of storage.

Table 3.6: Zeta potential value of freshly prepared SONs with different surfactant concentrations at 25 °C.

Surfactant Concentration (% ^{w/v})	Zeta Potential (mV)
0.25	-53.0 ± 0.5
0.50	-48.2 ± 0.3
1.00	-46.2 ± 0.4
1.50	-45.9 ± 0.5
2.00	-44.1 ± 0.9

3.2.2 Effect of Storage Temperature

Colloidal suspensions in general are thermodynamically unstable system and destabilization is easily stimulated by their surrounding temperature and pressure. Destabilization may occur due to the improper storage condition of SON particles especially at high temperature. Therefore, it is important to investigate the effect of temperature on stability of SON dispersions. In this study, SON dispersions were stored at 5 °C, room temperature (about 28 °C) and 45 °C, respectively and their mean particle sizes were determined by using dynamic light scattering technique at certain time intervals for 28 days. SONs also observed under TEM microscopy to visualise the change in the morphology.

The change in particle size of SON dispersions when stored at different temperatures is shown in Figure 3.7. There is almost no significant change in particle size for SON stored at 5 °C for 28 days. A gradual increase in particle size from 240 nm to 350 nm for SON stored at room temperature. This is in agreement the TEM micrographs that showed present of larger particles. Moreover, sedimentation of particles was also observed for SON dispersion that stored at room temperature as shown in Figure 3.8. However, SON dispersion which stored at 45 °C showed dramatically increased in mean particle size up to about one micron during 28 days of storage (Figure 3.7). Large and irregular spherical shape particles were also observed in TEM micrographs. A denser sedimentation of particles was also observed for sample stored at 45 °C (Figure 3.8). These observations indicated that the stability of SON suspension was greatly influent by the storage temperature. This could be explained that at elevated temperature, frequency of collision among particles increases and lower electrostatic repulsion between incoming particles lead to particle aggregation. Hence, this speeds up flocculation process that eventually leads to larger aggregates. Besides

the aggregation, the nanoparticles may be partially melted and fused to become large irregular shape particles.

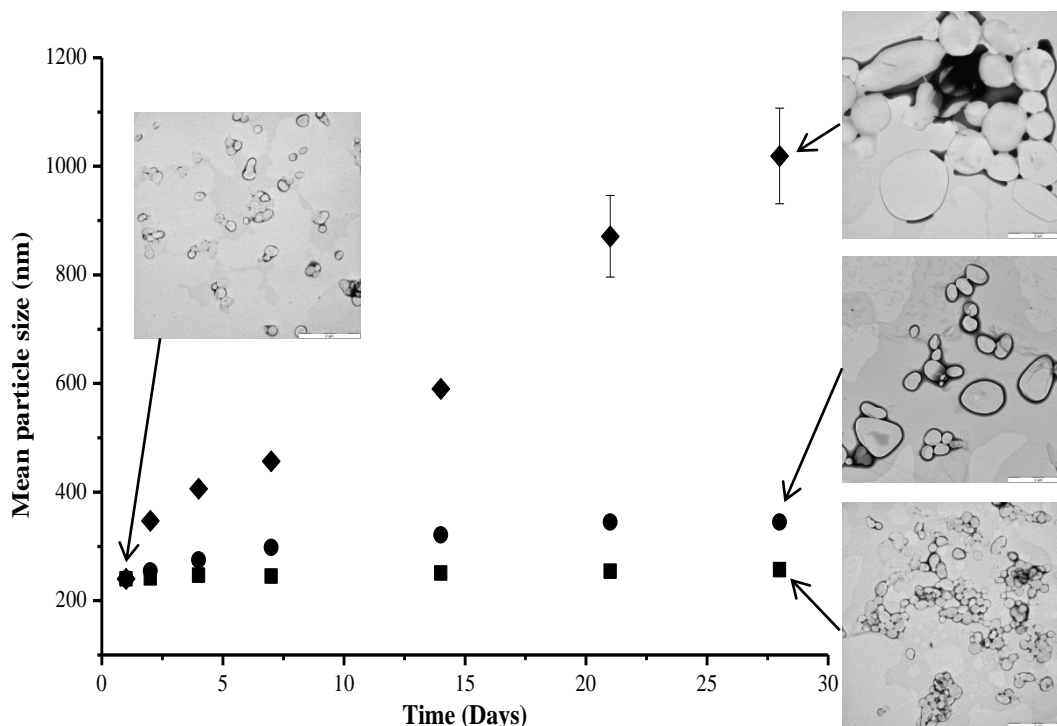


Figure 3.7: Plot of mean particle size of SON dispersions as function of storage time at 5 °C (■), room temperature (about 28 °C) (●) and 45 °C (◆) and the TEM micrographs showed the changes in shape of nanoparticles, scale bar is 1 μm .



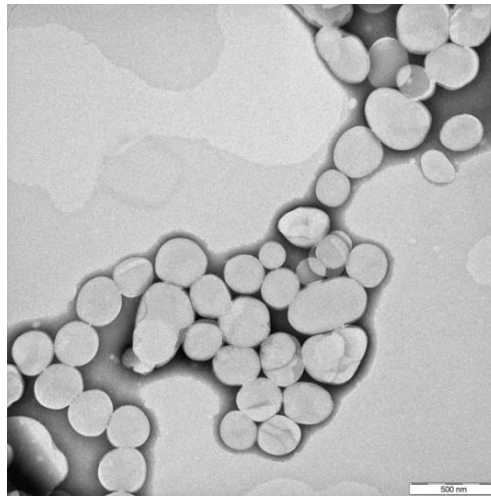
Figure 3.8: Photograph of SONs stored at different temperatures (a) 5 °C (left), (b) room temperature (middle) and (c) 45 °C (right) after 28 days showing denser sedimentation.

3.3 Effect of Oleic Acid Composition on the Morphologies of SONs

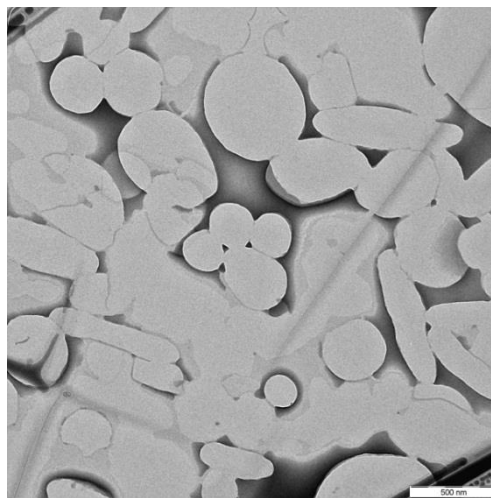
Oleic acid is in liquid form at room temperature. The present of oleic acid composition may disrupt the internal crystalline structure of stearic acid in SON particles. To visualize the effect of oleic acid composition on morphologies of nanoparticles, freshly prepared SONs were observed using TEM microscopy. Figure 3.9 showed the TEM micrographs of SONs with different oleic acid compositions. The morphology of SON without oleic acid appeared to be more monodisperse spherical shape and relatively small particle size.

When about 30 wt% of oleic acid in the compositions of SON, the particles appeared to be larger and starting to be elongate as shown in Figure 3.9 (b). When the oleic acid composition increased to 50 wt%, most of the particles appeared as elongated particles as shown in Figure 3.9 (c). The TEM micrographs revealed that the higher oleic acid composition led to the formation of elongated particles with larger particle size.

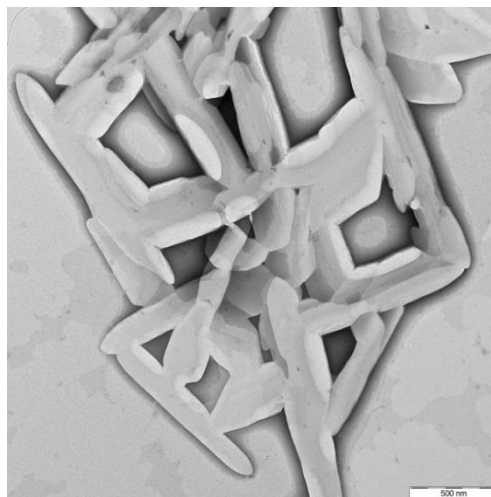
The surface area to volume ratio of elongated particles is assumed to be bigger as compared to spherical shape SON. The elongated particles are not preferable because its low surface area to volume ratio may limit the contact area of particles to be absorbed onto the skin surface. However, certain amount of oleic acid is needed to improve the encapsulation efficiency of SON. Therefore, it is not recommended to incorporate high amount of oleic acid into SON.



(a)



(b)



(c)

Figure 3.9: TEM micrographs of SONs. (a) SON without oleic acid, (b) SON with 30 wt% oleic acid composition, (c) SON with 50 wt% oleic acid composition, scale bar is 500 nm.

3.4 Differential Scanning Calorimetry (DSC)

DSC has been extensively employed in the lipid nanoparticles research to assess the thermal parameters such as melting point, melting enthalpy and degree of crystallinity. One of the features of lipid nanoparticles is they occur as rigid nanoparticles at both room temperature and body temperature and this unique property gives controlled release of payloads. To improve encapsulation efficiency of active ingredients, lipid nanoparticles were produce by mixing of solid lipid and oily lipid. However, addition of oily lipid into solid lipid matrix may change the overall melting parameters of the lipid nanoparticles. In this study, the effect of oleic acid concentration in the composition on melting behaviour of SON particles was investigated.

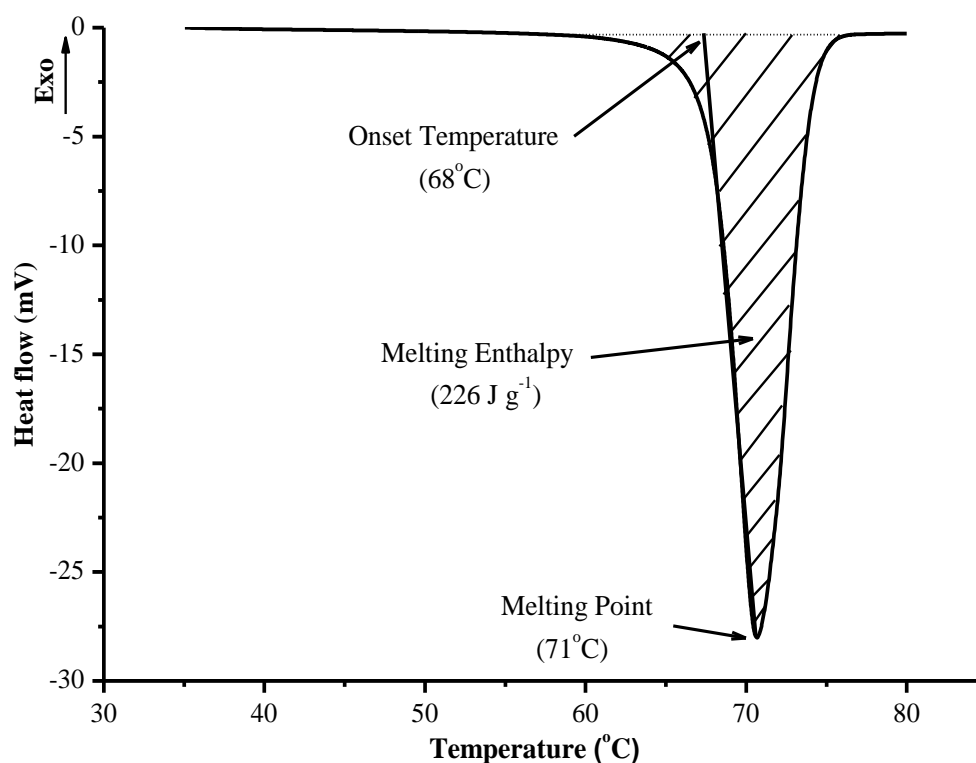


Figure 3.10: Endothermic thermogram of stearic acid at the heating rate of 5 °C min⁻¹.

Figure 3.10 showed the endothermic thermogram of stearic acid and the melting parameters such as melting point, onset temperature and melting enthalpy of stearic acid were analysed by using TA Universal Analysis software. The peak of the endothermic thermogram indicates the melting point of stearic acid and onset temperatures is obtained from the intersection of the tangent of the endothermic peak with the extrapolated baseline. The shaded area of the endothermic thermogram is proportional to the melting enthalpy of stearic acid which is 226 J g^{-1} .

All the endothermic thermograms of both salicylic acid and lidocaine loaded SONs showed one endothermic peak and the melting point shifts towards lower temperature accompanied by increasing in the width of the melting peak (Figure 3.111 and 3.12). The melting point of SON with salicylic acid gradually decreased about $12 \text{ }^{\circ}\text{C}$ from 0 wt% to 50 wt% oleic acid content (Table 3.7). Similar result was also obtained for SON with lidocaine. The melting point of SON with lidocaine also decreased about $17 \text{ }^{\circ}\text{C}$ as oleic acid composition increased from 0 wt% to 50 wt% (Table 3.8).

The degree of crystallinity of SONs was determined by calculating the ratio of SON melting enthalpy to stearic acid melting enthalpy as shown in the equation (4) at Section 2.7, Chapter 2. Taking the enthalpy of pure stearic acid at 226 J g^{-1} as 100%, the theoretical percentage of crystallinity of SONs with 10, 20, 30, 40 and 50 wt% oleic acid could then be obtained (Mühlen & Mehnert, 1998). The degree of crystallinity of SONs with salicylic acid was dramatically reduced about 60% with increasing oleic acid ratio from 0 wt% to 50 wt% (Table 3.7). Expectedly, the degree of crystallinity of SONs with lidocaine also was significantly decreased about 50% with increasing oleic acid ratio from 0 wt% to 50 wt% (Table 3.8). These could conclude that the present of oleic acid somehow perturb the stearic acid crystal matrix and increase the amorphous proportion in particles, leading to reduction in the degree of crystallinity of SONs.

Table 3.7: Onset temperatures (T_{onset}), melting points, melting enthalpies (ΔH) and degree of crystallinity of SONs with and without salicylic acid.

Oleic Acid Content (wt%)	Salicylic Acid loaded SONs			
	T_{onset} (°C)	Melting Point (°C)	ΔH (J/g)	Degree of Crystallinity (%)
0	65.9	68.8	188	83
10	63.1	67.2	158	70
20	59.9	65.5	119	53
30	55.8	62.9	98	43
40	49.0	59.2	78	35
50	44.2	56.5	60	27

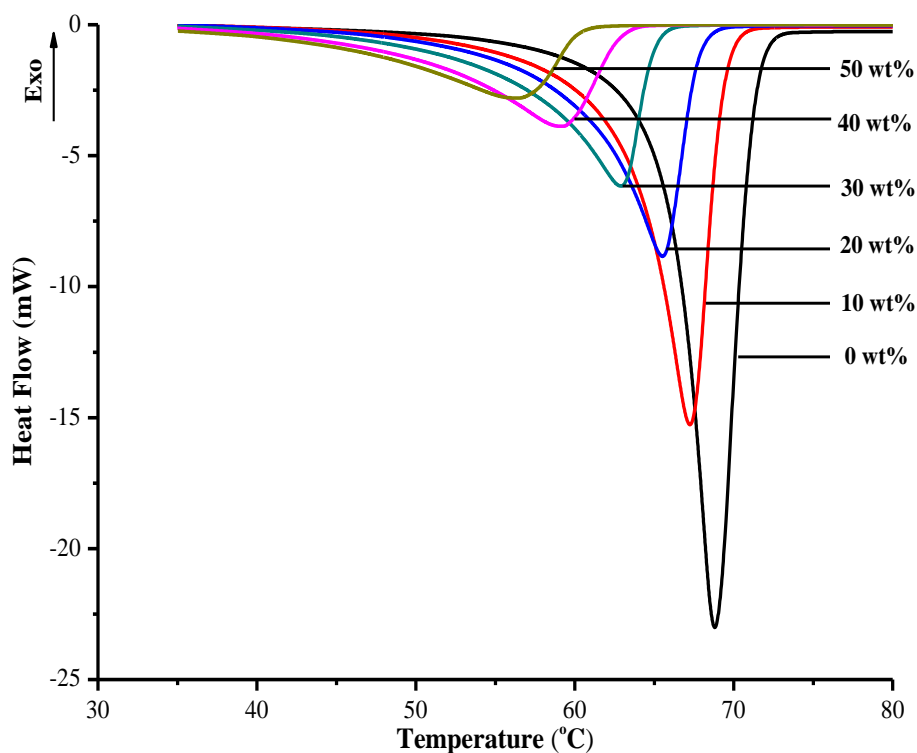


Figure 3.11: Endothermic thermograms of salicylic acid loaded SONs with 0 – 50 wt% oleic acid composition at the heating rate of 5 °C min^{-1} .

Table 3.8 Onset temperatures (T_{onset}), melting points, melting enthalpies (ΔH) and degree of crystallinity of SONs with and without lidocaine.

Oleic Acid Content (wt%)	Lidocaine loaded SONs			
	T_{onset} (°C)	Melting Point (°C)	ΔH (J/g)	Degree of Crystallinity (%)
0	65.3	69.0	178	79
10	62.1	67.1	160	71
20	59.2	65.2	136	61
30	55.4	62.8	115	51
40	50.5	60.2	98	44
50	48.0	58.3	73	32

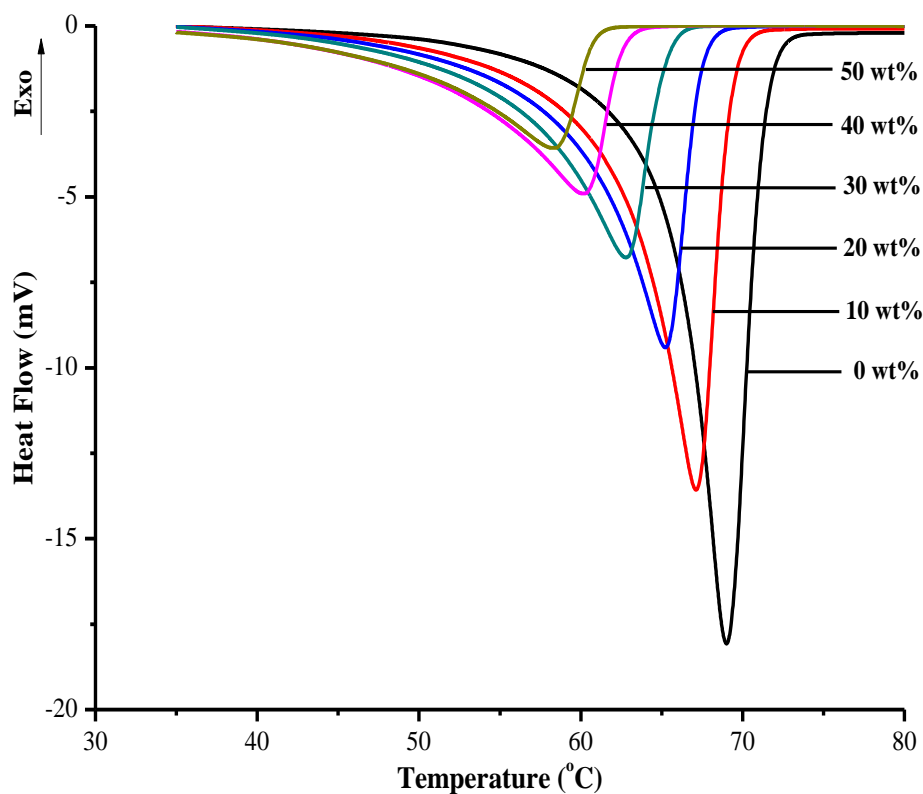


Figure 3.12: Endothermic thermograms of lidocaine loaded SONs with 0 – 50 wt% oleic acid composition at the heating rate of 5 °C min^{-1} .

3.5 Encapsulation Efficiency of SONS

For a carrier system, it is important to encapsulate the active ingredients as much as possible. In lipid nanoparticles research, one of the strategies to improve encapsulation efficiency of carrier is to produce the lipid nanoparticles with the mixture of liquid oil and solid lipid. In this study, SONS were prepared by mixture of stearic acid and oleic acid as mentioned in Chapter 2. The encapsulation efficiency of salicylic acid loaded SONS increased from 49% to 69% with increasing the oleic acid composition from 0 wt% to 40 wt%, respectively, but slightly decreased to 63% for 50 wt% oleic acid content as shown in Figure 3.13. A substantially increased in the encapsulation efficiency of lidocaine loaded SONS from 50% to 70% with increasing the oleic acid composition up to 30 wt% and subsequently remains around $\pm 70\%$ as oleic acid composition increased up to 50 wt%.

Encapsulation efficiency has always been correlated with the degree of crystallinity of lipid nanoparticles (Almeida *et al.*, 2012). It has been shown in previous section that the addition of oleic acid into SONS composition increases the amorphous state in the solid lipid matrix and decreases the overall particle crystallinity, thereby improves the encapsulation efficiency. This has been explained the reason of increased in encapsulation efficient of both active ingredients as amount of oleic acid in the mixture increased. Jennings *et al.* also reported that incorporation of liquid oil into lipid nanoparticles perturbed the crystalline matrix and results enough space to accommodate retinol molecules, thus increased the drug encapsulation capacity (Jennings *et al.*, 2000). This is further supported by Ribeiro *et al.* that encapsulation efficiency of lipid nanoparticles was directly proportional to the oleic acid concentration in the lipid phase (Ribeiro *et al.*, 2012).

However, the encapsulation efficiency of SONS containing large amount of oleic acid (50 wt%) slightly decreased which may be due to exclusion of oleic acid during crystallization of SONS that unable to incorporate higher amount of salicylic acid (Kim *et al.*, 2010; Lin *et al.*, 2007). On the other hand, the encapsulation efficiency of lidocaine loaded SONS remained around 70% owing the fact that lidocaine has higher preferential in lipid phase as compared to salicylic acid. Log *P* value is the indicator that showed the solubility of a particular compound in octane and water. Positive log *P* value indicated that a particular compound is preferable to dissolve in organic phase and vice versa. Lidocaine has higher log *P* value (2.44) as compared to salicylic acid which the log *P* value is around 2.26.

SONs with 30 wt%, 40 wt% and 50 wt% oleic acid composition demonstrated high loading efficiency of salicylic acid or lidocaine with similar sizes but SON with 30 wt% oleic acid content was considered as an optimized formulation because SONS with higher oleic acid concentration present as elongated solid particles that have lower melting behaviour and excess oleic acid content may easily oxidized especially when there is unexpected temperature fluctuation during storage and transportation.

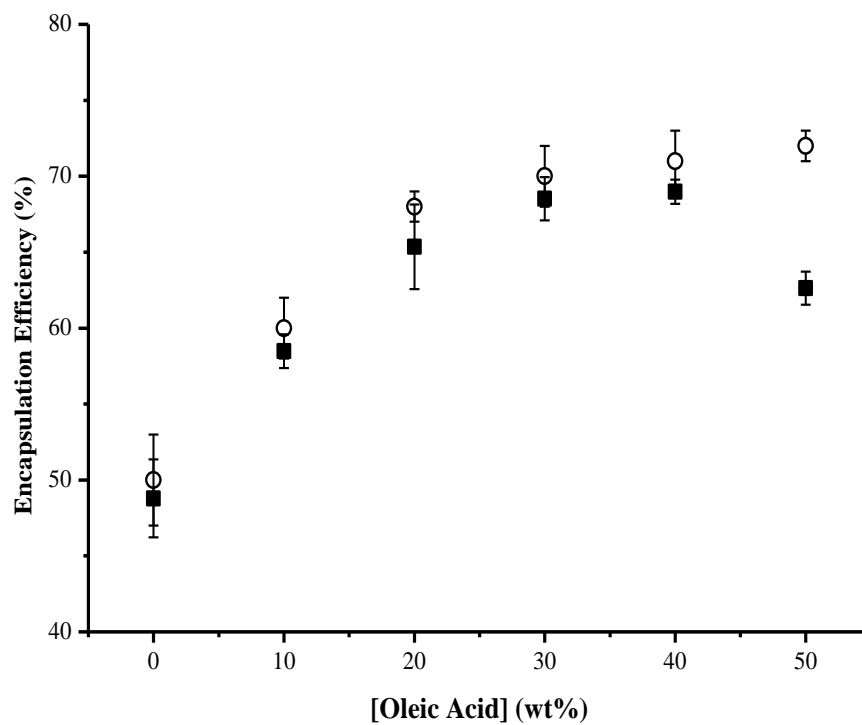


Figure 3.13: Plot of encapsulation efficiency of salicylic acid (■) and lidocaine (○) loaded SONs as function of oleic acid composition at 25 °C.

3.6 *In Vitro* Release Evaluation

SON with 30 wt% oleic acid content was selected owing to its optimum formulation property based on the results obtained from our particle size, morphology, thermal behaviour and encapsulation efficiency analysis. It was then further incorporated into a cream formulation for the *in vitro* release investigation.

Eight different samples as described in Section 2.11 were evaluated using Franz Diffusion Cell system and the cumulative amount of salicylic acid or lidocaine release from all samples were plotted against time as shown in Figure 3.14 and Figure 3.15, respectively. Sample A to D are the samples containing salicylic acid whereas Sample E to H are samples containing lidocaine. For samples containing salicylic acid, Samples A showed a rapid release within 8 hours whereas the Sample B, C and D demonstrated a biphasic release pattern whereby a rapid release of salicylic acid was observed in the first 8 hours followed by slower release at almost a constant rate (Figure 3.14). The initial fast release rates of Sample B, C and D could be due to the presence of free salicylic acid molecules in the aqueous phase which diffuse rapidly through the membrane. After the completion of the first phase of free salicylic acid within the first 8 hours, it is followed by the second phase which is much slower release rate that could be due to the retention of salicylic acid in the SON particle dispersion and/or in the emulsion. Sample C and D have slower release behaviour as compared to the samples without SON. The presence of controlled release behaviour for samples containing SON (Sample C and D) revealed that the salicylic acid molecules were successfully incorporated in the solid matrix of SON and slowly release from the particles. Similar results were also obtained for samples containing lidocaine. Sample E has substantially released within 6 hours whereas Sample F, G and H showed a faster rate of release followed by slower rate of release (Figure 3.15).

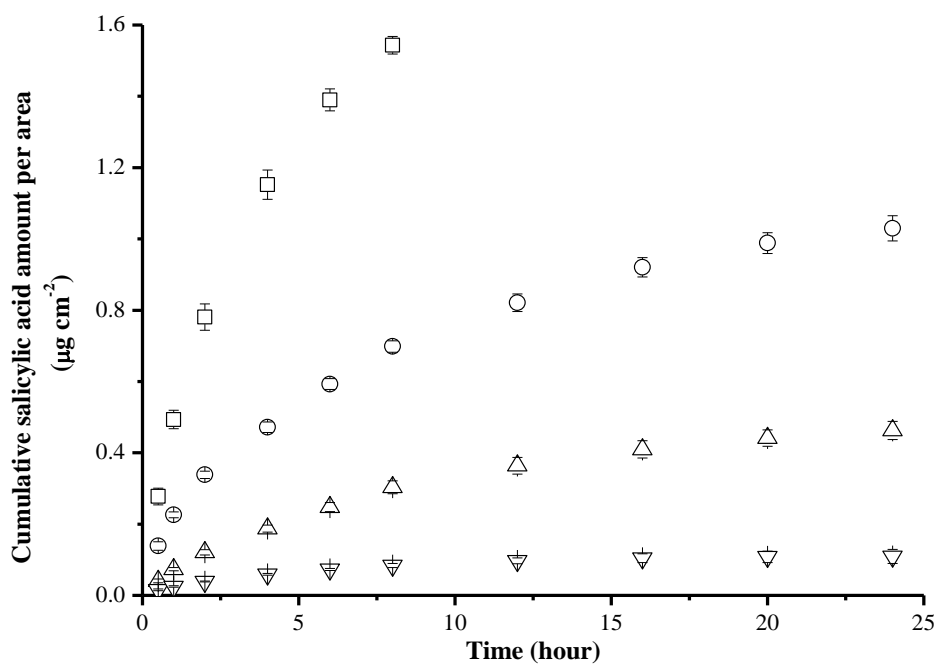


Figure 3.14: *In vitro* release study of salicylic acid solution (□), salicylic acid cream (○), salicylic acid loaded SON with 30 wt% oleic acid composition (△) and salicylic acid loaded SON with 30 wt% oleic acid composition in cream (▽) over a period of 24 hours at 37 °C.

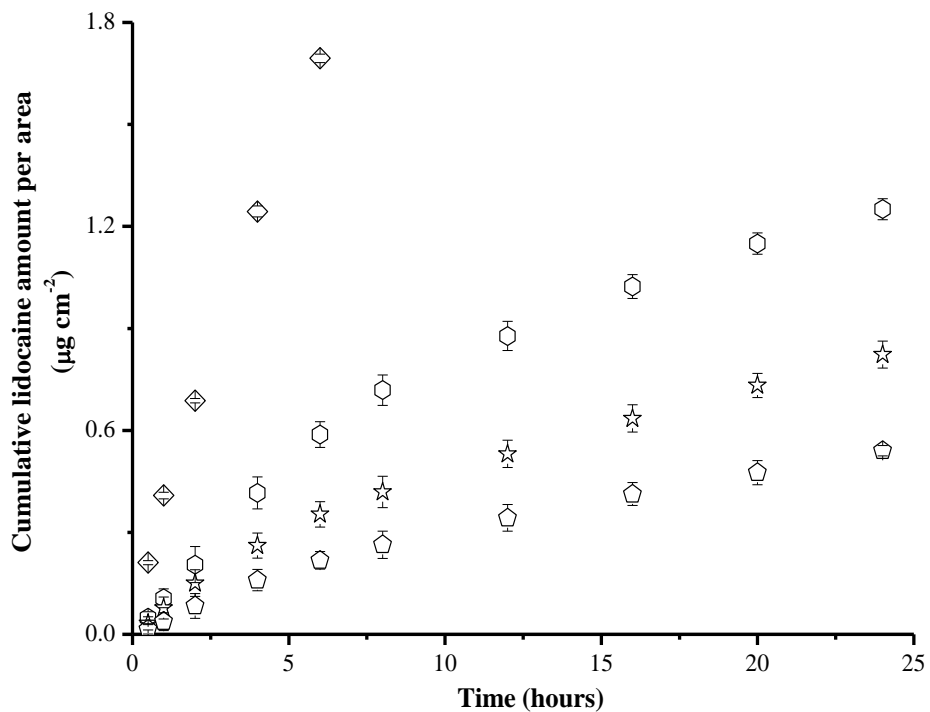


Figure 3.15: *In vitro* release study of lidocaine solution (◇), lidocaine cream (⊕), lidocaine loaded SON with 30 wt% oleic acid composition (★) and lidocaine loaded SON with 30 wt% oleic acid composition in cream (⊖) over a period of 24 hours at 37 °C.

In order to understand their release kinetic, the *in vitro* releases of the eight different samples were curve fitted to zero order, first order and Higuchi model. We have chosen the Higuchi model because it could describe diffusion of drug from homogenous and granular matrix system (Vivek *et al.*, 2007). The release profiles of the eight samples showed the best fit into Higuchi model ($R^2 > 0.95 - 0.99$) (Table 3.9). The linear fits of all samples indicated that the release of salicylic acid or lidocaine from the samples was diffusion controlled process (Vivek *et al.*, 2007).

Table 3.9: Different kinetic model evaluations of payloads (salicylic acid or lidocaine) release for eight different samples at 37C.

Sample	Zero Order		First Order		Higuchi Model	
	Slope	R ²	Slope	R ²	Slope	R ²
A	10.5	0.93	0.20	0.77	38.4	0.99
B	2.4	0.89	0.07	0.69	14.4	0.98
C	1.8	0.92	0.08	0.70	10.5	0.99
D	0.9	0.81	0.02	0.62	5.2	0.95
E	15.8	0.98	0.34	0.83	50.8	0.99
F	4.0	0.96	0.11	0.67	22.9	0.99
G	2.2	0.93	0.11	0.65	12.6	0.99
H	1.4	0.97	0.12	0.65	8.0	0.99

The slopes which obtained from the plotting of Higuchi model (Table 3.9) represent the release rate of payload (Shah & Hanson, 2003). The release rates of samples containing salicylic acid were followed the sequence of Sample A > B > C > D and the release rates of samples containing lidocaine were Sample E > F > G > H. The release rate of Sample A and E (solution form) were reduced after formulated into cream (Sample B and F) revealed this retentional effect by the emulsion. For cream that containing SON with salicylic acid or lidocaine (Sample D and H), the release rates were further decreased to about 3 times as compared to cream formulations (Sample B and F) and it is indicating that the SON prepared in this study has slow release property.

This slow release property of SON could be due to the release of active ingredients from the solid matrix of SON particle which involved two pathways as illustrated in Figure 3.16. In the retentate chamber, the payloads slowly released (k_1) from the particles to the aqueous phase and then diffused through the membrane at the faster rate (k_2) (Figure 3.16). The reason of slow release of payloads at the first pathway may be due to the hydrophobic solid matrix of SON retards the release of salicylic acid or lidocaine to the aqueous phase, thus results in slower release rate.

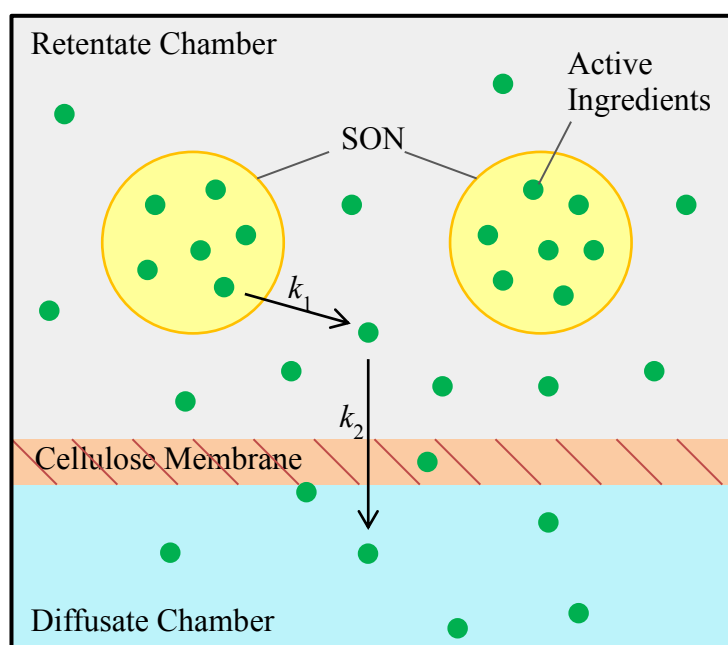


Figure 3.16: Schematic diagram for *in vitro* release mechanism of SON with active ingredients in Franz Diffusion Cell.

CHAPTER 4

CONCLUSION

4.1 Conclusion

A series of SONs were successfully prepared by using melt-emulsification combined with ultrasonication method and a series of experiments were carried out to investigate the influence of device parameters such as speed and time of homogenization and period of sonication in order to obtain smaller particles with narrow size distributions. The optimized preparation parameters of SONs are homogenizing at 15000 rpm for 300 s and followed by 120 s of sonication.

It was also found that the SON compositions such as lipid content, surfactant concentration and amount of active ingredients directly influenced the particle size of nanoparticles. The size of nanoparticles was increased linearly with increased in the lipid content. The particle size also varied with the oleic acid composition in the mixture. At the same time, TEM images showed that higher amount of oleic acid concentration in the mixture led to formation of elongated SON particles. On the other hands, small size of nanoparticles could be obtained by increasing the amount of surfactant in SON. The participation of active ingredients in formation of SON particles also resulted larger particles. The prepared nanoparticles with both salicylic acid and lidocaine possessed a mean particle size of about 250 nm to 330 nm. The stability of SONs was also evaluated by monitoring the change of particle size of SON which stored at different temperatures (5 °C, room temperature and 45 °C). The results showed that the particle size of SON maintained stable at 5 °C for 4 weeks.

Encapsulation efficiency for salicylic acid and lidocaine increased from 50% to 70% with increasing amount of oleic acid into SON composition. This could be explained by the results of DSC analysis which was showed that the decreased in degree of crystallinity of SONs with increasing oleic acid composition in the mixture. Different amount of oleic acid mixed gave different degree of perturbation to the crystalline

matrix of SONs hence result in lower degrees of crystallinity, thereby improve their encapsulation efficiencies. SON with 30 wt% oleic acid content was considered as an optimized formulation because it demonstrated high loading efficiency for both salicylic acid and lidocaine with similar sizes.

In vitro release of salicylic acid or lidocaine in samples such as solution, cream, SON dispersion and SON into the cream was evaluated by using Franz Diffusion Cell technique. The *in vitro* release study showed that SON dispersion performed a gradual release for 24 hours as compared to its solution form and cream, denoting the incorporation of salicylic acid or lidocaine in solid matrix of SON and prolonged the *in vitro* release. Both salicylic acid and lidocaine in cream formulation which containing SONs has about 3 times slower release rate as compared to its solution form, suggesting the potential use of SON as carrier to improve therapeutic efficacy in cosmetic and pharmaceutical products.

REFERENCES

References

- Almeida, E. D. P., Costa, A. A., Serafini, M. R., Rossetti, F. C., Marchetti, J. M., Sarmiento, V. H. V., Nunes, R. D. S., ... Lira, A. A. M. (2012). Preparation and characterization of chloroaluminum phthalocyanine-loaded solid lipid nanoparticles by thermal analysis and powder X-ray diffraction techniques. *Journal of Thermal Analysis and Calorimetry*, *108*(1), 191-196. doi: 10.1007/s10973-011-1868-z
- Anton, N., Benoit, J.-P., & Saulnier, P. (2008). Design and production of nanoparticles formulated from nano-emulsion templates—a review. *Journal of Controlled Release*, *128*(3), 185-199.
- Arda, O., Göksüğüür, N., & Tüzün, Y. (2014). Basic histological structure and functions of facial skin. *Clinics in Dermatology*, *32*(1), 3-13. doi: <http://dx.doi.org/10.1016/j.clindermatol.2013.05.021>
- Awad, T. S., Helgason, T., Weiss, J., Decker, E. A., & McClements, D. J. (2009). Effect of omega-3 fatty acids on crystallization, polymorphic transformation and stability of tripalmitin solid lipid nanoparticle suspensions. *Crystal Growth and Design*, *9*(8), 3405-3411.
- Barry, B. W. (1983). *Dermatological formulations : Percutaneous absorption*. New York: Marcel Dekker.
- Benson, H. A. (2000). Assessment and clinical implications of absorption of sunscreens across skin. *American Journal of Clinical Dermatology*, *1*(4), 217-224.
- Bensouilah, J., & Buck, P. (2006). *Aromadermatology: aromatherapy in the treatment and care of common skin conditions*: Radcliffe Publishing.
- Bhaskar, K., Anbu, J., Ravichandiran, V., Venkateswarlu, V., & Rao, Y. M. (2009). Lipid nanoparticles for transdermal delivery of flurbiprofen: Formulation, in vitro, ex vivo and in vivo studies. *Lipids in Health and Disease*, *8*. doi: 10.1186/1476-511x-8-6
- Brisson, P. (1974). Percutaneous absorption. *Canadian Medical Association Journal*, *110*(10), 1182.
- Bunjes, H., & Unruh, T. (2007). Characterization of lipid nanoparticles by differential scanning calorimetry, X-ray and neutron scattering. *Advanced Drug Delivery Reviews*, *59*(6), 379-402. doi: <http://dx.doi.org/10.1016/j.addr.2007.04.013>
- Castro, G. A., Orđice, R. L., Vilela, J. M. C., Andrade, M. S., & Ferreira, L. A. M. (2007). Development of a new solid lipid nanoparticle formulation containing retinoic acid for topical treatment of acne. *Journal of Microencapsulation*, *24*(5), 395-407.
- Chattopadhyay, P., Shekunov, B. Y., Yim, D., Cipolla, D., Boyd, B., & Farr, S. (2007). Production of solid lipid nanoparticle suspensions using supercritical fluid extraction of emulsions (SFEE) for pulmonary delivery using the AERx system. *Advanced Drug Delivery Reviews*, *59*(6), 444-453.

- Das, S., Ng, W. K. & Tan, R. B. (2012). Are nanostructured lipid carriers (NLCs) better than solid lipid nanoparticles (SLNs): Development, characterizations and comparative evaluations of clotrimazole-loaded SLNs and NLCs? *European Journal of Pharmaceutical Sciences*, 47(1), 139-151. doi: <http://dx.doi.org/10.1016/j.ejps.2012.05.010>
- Davis, S. S., Washington, C., West, P., Illum, L., Liversidge, G., Sternson, L., & Kirsh, R. (1987). Lipid emulsions as drug delivery systems. *Annals of the New York Academy of Sciences*, 507(1), 75-88.
- Denke, M. (1994). Role of beef and beef tallow, an enriched source of stearic acid, in a cholesterol-lowering diet. *The American journal of clinical nutrition*, 60(6), 1044S-1049S.
- Domb, A., & Maniar, M. (1991). Lipospheres for controlled delivery of substances: Wo Patent 1,991,007,171.
- Edwards, C., & Marks, R. (1995). Evaluation of biomechanical properties of human skin. *Clinics in Dermatology*, 13(4), 375-380.
- Finkel, Y., Bolme, P., & Eriksson, M. (1981). The effect of food on the oral absorption of penicillin V preparations in children. *Acta Pharmacologica et Toxicologica*, 49(4), 301-304. doi: 10.1111/j.1600-0773.1981.tb00910.x
- Franzetti, A., Gandolfi, I., Bestetti, G., & Banat, I. (2010). (Bio)surfactant and bioremediation, successes and failures. In G. Plaza (Eds.), *Trending in bioremediation and phytoremediation* (pp. 145-156). Kerala, India: Research Signpost.
- Gasco, M. R. (1993). Method for producing solid lipid microspheres having a narrow size distribution: Google Patents.
- Gaur, P. K., Mishra, S., & Purohit, S. (2013). Solid lipid nanoparticles of guggul lipid as drug carrier for transdermal drug delivery. *BioMed Research International*, 2013, 10. doi: 10.1155/2013/750690
- Geerligs, M. (2010). *Skin layer mechanics*. Doctoral Thesis, TU Eindhoven, Netherlands.
- Graham, C. W., Pagano, R. R., & Katz, R. L. (1977). Thrombophlebitis after intravenous diazepam—Can it be prevented? *Anesthesia & Analgesia*, 56(3), 409-413.
- Guimarães, K. L., & Ré M. I. (2011). Lipid nanoparticles as carriers for cosmetic ingredients: The first (SLN) and the Second Generation (NLC) *Nanocosmetics and Nanomedicines* (pp. 101-122): Springer.
- Han, F., Li, S., Yin, R., Liu, H. & Xu, L. (2008). Effect of surfactants on the formation and characterization of a new type of colloidal drug delivery system: Nanostructured lipid carriers. *Colloids and Surfaces A: Physicochemical and Engineering Aspects*, 315(1-3), 210-216. doi: 10.1016/j.colsurfa.2007.08.005

- Hu, F. Q., Jiang, S. P., Du, Y. Z., Yuan, H., Ye, Y. Q. & Zeng, S. (2005). Preparation and characterization of stearic acid nanostructured lipid carriers by solvent diffusion method in an aqueous system. *Colloids and Surfaces B: Biointerfaces*, 45(3-4), 167-173. doi: 10.1016/j.colsurfb.2005.08.005
- Jayaraman, S. C., Ramachandran, C., & Weiner, N. (1996). Topical delivery of erythromycin from various formulations: an in vivo hairless mouse study. *Journal of Pharmaceutical Sciences*, 85(10), 1082-1084.
- Jafari, S. M., He, Y., & Bhandari, B. (2006). Nano-emulsion production by sonication and microfluidization—a comparison. *International Journal of Food Properties*, 9(3), 475-485.
- Jenning, V., & Gohla, S. H. (2001). Encapsulation of retinoids in solid lipid nanoparticles (SLN[®]). *Journal of Microencapsulation*, 18(2), 149-158. doi: 10.1080/02652040010000361
- Jenning, V., Schäfer-Korting, M., & Gohla, S. H. (2000). Vitamin A loaded solid lipid nanoparticles for topical use drug release properties. *Journal of Controlled Release* 66, 115–126.
- Jenning, V., Thünemann, A. F., & Gohla, S. H. (2000). Characterisation of a novel solid lipid nanoparticle carrier system based on binary mixtures of liquid and solid lipids. *International Journal of Pharmaceutics*, 199(2), 167-177. doi: [http://dx.doi.org/10.1016/S0378-5173\(00\)00378-1](http://dx.doi.org/10.1016/S0378-5173(00)00378-1)
- Jenning, V., Gysler, A., Schäfer-Korting, M., & Gohla, S. H. (2000). Vitamin A loaded solid lipid nanoparticles for topical use: occlusive properties and drug targeting to the upper skin. *European Journal of Pharmaceutics and Biopharmaceutics*, 49(3), 211-218.
- Kanitakis, J. (2002). Anatomy, histology and immunohistochemistry of normal human skin. *European Journal of Dermatology*, 12(4), 390-399.
- Kheradmandnia, S., Vasheghani-Farahani, E., Nosrati, M. & Atyabi, F. (2010). Preparation and characterization of ketoprofen-loaded solid lipid nanoparticles made from beeswax and carnauba wax. *Nanomedicine: Nanotechnology, Biology, and Medicine*, 6(6), 753-759. doi: 10.1016/j.nano.2010.06.003
- Kim, J. K., Park, J. S. & Kim, C. K. (2010). Development of a binary lipid nanoparticles formulation of itraconazole for parenteral administration and controlled release. *International Journal of Pharmaceutics*, 383(1-2), 209-215.
- Krutmann, J., & Humbert, P. (2011). *Nutrition for healthy skin*: Springer-Verlag Berlin Heidelberg.
- Kwatra, S., Taneja, G., & Nasa, N. (2012). Alternative routes of drug administration—transdermal, pulmonary & parenteral. *Indo Global Journal of Pharmaceutical Sciences*, 2(4), 409-426.

- Lai-Cheong, J. E., & McGrath, J. A. (2013). Structure and function of skin, hair and nails. *Medicine*, 41(6), 317-320. doi: <http://dx.doi.org/10.1016/j.mpmed.2013.04.017>
- Leng, F., Wan, J., Liu, W., Tao, B., & Chen, X. (2012). Prolongation of epidural analgesia using solid lipid nanoparticles as drug carrier for lidocaine. *Regional Anesthesia and Pain Medicine*, 37(2), 159-165.
- Leray, C. (2012). *Introduction to Lipidomics: From Bacteria to Man*: CRC Press.
- Lin, X., Li, X., Zheng, L., Yu, L., Zhang, Q. & Liu, W. (2007). Preparation and characterization of monocaprates nanostructured lipid carriers. *Colloids and Surfaces A: Physicochemical and Engineering Aspects*, 311(1-3), 106-111.
- Lucks, J. S., & Müller, R. H. (1991). EP 0000605497.
- Maia, C. S., Mehnert, W., & Schäfer-Korting, M. (2000). Solid lipid nanoparticles as drug carriers for topical glucocorticoids. *International Journal of Pharmaceutics*, 196(2), 165-167.
- Mangold, H. K. (1995). The Lipid Handbook, 2nd Edition, F. D. Gunstone, J. L. Harwood and F. B. Padley, Chapman & Hall, London, 315-316. doi: 10.1002/lipi.19950970720
- McClements, D. J. (1998). *Food emulsions: principles, practice, and techniques*: CRC press.
- Mehnert, W., & Mäder, K. (2012). Solid lipid nanoparticles: Production, characterization and applications. *Advanced Drug Delivery Reviews*, 64, Supplement(0), 83-101. doi: <http://dx.doi.org/10.1016/j.addr.2012.09.021>
- Mehta, R. (2000). Topical and transdermal drug delivery: what a pharmacist needs to know. *Midwestern University College of Pharmacy-Glendale, ACPE ID* (146-000), 01-008.
- Moody, M. L. (2010). Topical medications in the treatment of pain. *Pain Medicine News Special Edition*, 15-21.
- Mozafari, M. R. (2006). *Nanocarrier technologies: frontiers of nanotherapy*: Springer Dordrecht.
- Mühlen, A., Schwarz, C. & Mehnert, W. (1998). Solid lipid nanoparticles (SLN) for controlled drug delivery - Drug release and release mechanism. *European Journal of Pharmaceutics and Biopharmaceutics*, 45(2), 149-155. doi: 10.1016/s0939-6411(97)00150-1
- Müller, R. H. & Heinemann, S. (1994). Fat emulsions for parenteral nutrition. IV. Lipofundin MCT/LCT regimens for total parenteral nutrition (TPN) with high electrolyte load. *International Journal of Pharmaceutics*, 107(2), 121-132.

- Müller, R. H., Jacobs, C. & Kayser, O. (2001). Nanosuspensions as particulate drug formulations in therapy: Rationale for development and what we can expect for the future. *Advanced Drug Delivery Reviews*, 47(1), 3-19. doi: 10.1016/s0169-409x(00)00118-6
- Müller, R. H., Mehnert, W., Lucks, J. S., Schwarz, C., Muhlen, A., Weyhers, H., ... Ruhl, D. (1995). Solid lipid nanoparticles (SLN) - An alternative colloidal carrier system for controlled drug delivery. *European Journal of Pharmaceutics And Biopharmaceutics*, 41(1), 62-69.
- Nyenwe, E. A., Jerkins, T. W., Umpierrez, G. E., & Kitabchi, A. E. (2011). Management of type 2 diabetes: evolving strategies for the treatment of patients with type 2 diabetes. *Metabolism*, 60(1), 1-23.
- Pardeike, J., Hommoss, A., & Müller, R. H. (2009). Lipid nanoparticles (SLN, NLC) in cosmetic and pharmaceutical dermal products. *International Journal of Pharmaceutics*, 366(1-2), 170-184. doi: <http://dx.doi.org/10.1016/j.ijpharm.2008.10.003>
- Pardeike, J., & Müller, R. H. (2007). Coenzyme Q10-loaded NLCs: Preparation, occlusive properties and penetration enhancement. *Pharmaceutical Technology Europe*, 19(7), 46-49.
- Pathak, P., & Nagarsenker, M. (2009). Formulation and evaluation of lidocaine lipid nanosystems for dermal delivery. *AAPS PharmSciTech*, 10(3), 985-992.
- Paudel, K. S., Milewski, M., Swadley, C. L., Brogden, N. K., Ghosh, P., & Stinchcomb, A. L. (2010). Challenges and opportunities in dermal/transdermal delivery. *Therapeutic delivery*, 1(1), 109-131.
- Priano, L., Esposti, D., Esposti, R., Castagna, G., De Medici, C., Fraschini, F., ... & Mauro, A. (2007). Solid lipid nanoparticles incorporating melatonin as new model for sustained oral and transdermal delivery systems. *Journal of Nanoscience and Nanotechnology*, 7(10), 3596-3601.
- Puglia, C., Sarpietro, M. G., Bonina, F., Castelli, F., Zammataro, M., & Chiechio, S. (2011). Development, characterization, and in vitro and in vivo evaluation of benzocaine- and lidocaine-loaded nanostructured lipid carriers. *Journal of Pharmaceutical Sciences*, 100(5), 1892-1899.
- Raffa, R. B. (2010). Drug disposition and response. *Handbook of Drug-nutrient Interactions* (pp. 27-43). New York, NY: Springer.
- Ramasamy, T., Khandasami, U. S., Ruttala, H., & Shanmugam, S. (2012). Development of solid lipid nanoparticles enriched hydrogels for topical delivery of anti-fungal agent. *Macromolecular Research*, 20(7), 682-692.
- Riangjanapatee, P., & Okonogi, S. (2012). Effect of surfactant on lycopene-loaded nanostructured lipid carriers. *Drug Discoveries & Therapeutics*, 6(3).

- Ribeiro, M. D. M. M., Arellano, D. B. & Grosso, C. R. F. (2012). The effect of adding oleic acid in the production of stearic acid lipid microparticles with a hydrophilic core by a spray-cooling process. *Food Research International*, 47(1), 38-44. doi: <http://dx.doi.org/10.1016/j.foodres.2012.01.007>
- Scalia, S., Coppi, G., & Iannuccelli, V. (2011). Microencapsulation of a cyclodextrin complex of the UV filter, butyl methoxydibenzoylmethane: In vivo skin penetration studies. *Journal of Pharmaceutical and Biomedical Analysis*, 54(2), 345-350. doi: 10.1016/j.jpba.2010.09.018
- Schlupp, P., Blaschke, T., Kramer, K. D., Hötje, H. D., Mehnert, W., & Schäfer-Korting, M. (2011). Drug release and skin penetration from solid lipid nanoparticles and a base cream: a systematic approach from a comparison of three glucocorticoids. *Skin Pharmacology and Physiology*, 24(4), 199-209.
- Schwarz, J. C., Baisaeng, N., Hoppel, M., Löw, M., Keck, C. M., & Valenta, C. (2013). Ultra-small NLC for improved dermal delivery of coenzyme Q10. *International Journal of Pharmaceutics*, 447(1-2), 213-217. doi: <http://dx.doi.org/10.1016/j.ijpharm.2013.02.037>
- Shah, V. P., Elkins, J., Shaw, S., & Hanson, R. (2003). In vitro release: comparative evaluation of vertical diffusion cell system and automated procedure. *Pharmaceutical Development And Technology*, 8(1), 97-102. doi: [doi:10.1081/PDT-120017528](http://dx.doi.org/10.1081/PDT-120017528)
- Simopoulos, A. P. (1991). Omega-3 fatty acids in health and disease and in growth and development. *The American Journal of Clinical Nutrition*, 54(3), 438-463.
- Smoller, B. R., & Hiatt, K. M. (2009). *Dermatopathology: the basics*: Springer.
- Sobanko, J. F., Miller, C. J., & Alster, T. S. (2012). Topical anesthetics for dermatologic procedures: a review. *Dermatologic Surgery: Official Publication for American Society for Dermatologic Surgery [Et Al.]*, 38(5), 709-721. doi: [10.1111/j.1524-4725.2011.02271.x](http://dx.doi.org/10.1111/j.1524-4725.2011.02271.x)
- Souto, E., Mehnert, W., & Müller, R. (2006). Polymorphic behaviour of Compritol® 888 ATO as bulk lipid and as SLN and NLC. *Journal of Microencapsulation*, 23(4), 417-433.
- Souto, E., & Müller, R. H. (2007). Rheological and in vitro release behaviour of clotrimazole-containing aqueous SLN dispersions and commercial creams. *Die Pharmazie-An International Journal of Pharmaceutical Sciences*, 62(7), 505-509.
- Souto, E. B., Wissing, S. A., Barbosa, C. M. & Müller, R. H. (2004). Development of a controlled release formulation based on SLN and NLC for topical clotrimazole delivery. *International Journal of Pharmaceutics*, 278(1), 71-77. doi: <http://dx.doi.org/10.1016/j.ijpharm.2004.02.032>
- Speiser, P. (1990). Lipid nano pellets as drug carriers for oral administration: EP Patent 0,167,825.

- Stillwell, W. (2013). *An Introduction to Biological Membranes: From Bilayers to Rafts*: Newnes.
- Tadros, T. F. (2006). *Applied surfactants*: Wiley. com.
- Teeranachaideekul, V., Souto, E. B., Junyaprasert, V. B., & Müller, R. H. (2007). Cetyl palmitate-based NLC for topical delivery of Coenzyme Q 10—Development, physicochemical characterization and *in vitro* release studies. *European Journal of Pharmaceutics and Biopharmaceutics*, 67(1), 141-148.
- Tenjarla, S. (1999). Microemulsions: an overview and pharmaceutical applications. *Critical Reviews™ in Therapeutic Drug Carrier Systems*, 16(5).
- Tsai, M. J., Wu, P. C. Huang, Y. B. Chang, J. S. Lin, C. L. Tsai, Y. H., & Fang, J. Y. (2012). Baicalein loaded in tocol nanostructured lipid carriers (tocol NLCs) for enhanced stability and brain targeting. *International Journal of Pharmaceutics*, 423(2), 461-470. doi: 10.1016/j.ijpharm.2011.12.009
- Umbreit, J. N., & Strominger, J. L. (1973). Relation of detergent HLB number to solubilization and stabilization of D-alanine carboxypeptidase from *Bacillus subtilis* membranes. *Proceedings of the National Academy of Sciences*, 70(10), 2997-3001.
- Üner, M., Wissing, S. A., Yener, G., & Müller, R. H. (2005). Skin moisturizing effect and skin penetration of ascorbyl palmitate entrapped in Solid Lipid Nanoparticles (SLN) and Nanostructured Lipid Carriers (NLC) incorporated into hydrogel. *Pharmazie*, 60(10), 751-755.
- Vinnars, E., & Hammarqvist, F. (2004). 25th Arvid Wretling's Lecture—Silver anniversary, 25 years with ESPEN, the history of nutrition. *Clinical Nutrition*, 23(5), 955-962. doi: <http://dx.doi.org/10.1016/j.clnu.2004.06.001>
- Vivek, K., Reddy, L. H., & Murthy, R. S. R. (2007). Investigations of the effect of the lipid matrix on drug entrapment, *in vitro* release, and physical stability of olanzapine-loaded solid lipid nanoparticles. *AAPS PharmSciTech*, 8(4), E83-E83. doi: 10.1208/pt0804083
- Vivek, K., Reddy, L. H., & Murthy, R. S. R. (2007). Comparative study of some biodegradable polymers on the entrapment efficiency and release behavior of etoposide from microspheres. *Pharmaceutical Development And Technology*, 12(1), 79-88.
- Watson, A. D. J. (1986). Influence of food on absorption of antimicrobial drugs. In A. S. J. P. A. M. Miert, M. G. Bogaert & M. Debackere (Eds.), *Comparative Veterinary Pharmacology, Toxicology and Therapy* (pp. 93-104): Springer Netherlands.
- Wiechers, J. W. (1989). The barrier function of the skin in relation to percutaneous absorption of drugs. *Pharmaceutisch Weekblad*, 11(6), 185-198. doi: 10.1007/bf01959410

- Wilkes, G. L., Brown, I. A., & Wildnauer, R. H. (1973). The biomechanical properties of skin. *CRC Critical Reviews In Bioengineering*, 1(4), 453-495.
- Williams, A. (2003). *Transdermal and topical drug delivery: From theory to clinical practice*. London: Pharmaceutical Press.
- Wissing, S. A., Kayser, O., & Müller, R. H. (2004). Solid lipid nanoparticles for parenteral drug delivery. *Advanced Drug Delivery Reviews*, 56(9), 1257-1272. doi: <http://dx.doi.org/10.1016/j.addr.2003.12.002>
- Woo, J. O., Misran, M., Lee, P. F., & Tan, L. P. (2014). Development of a controlled release of salicylic acid loaded stearic acid-oleic acid nanoparticles in cream for topical delivery. *The Scientific World Journal*, 2014, 7. doi: 10.1155/2014/205703
- Zaidi, Z., & Lanigan, S. W. (2010). Skin: structure and function. *Dermatology in Clinical Practice* (pp. 1-15): Springer.